The Abdus Salam
International Centre
for Theoretical Physics

2359-11

**Joint ICTP-IAEA Workshop on Physics of Radiation Effect and its Simulation for Non-Metallic Condensed Matter**

*13 - 24 August 2012*

# Radiation damage in nuclear materials ITU approach

Thierry Wiss

*Joint Research Centre, European Commission*
*Eggenstein*
*Germany*

Commission européenne

# Radiation damage in nuclear materials ITU approach

**Thierry WISS**

The European Commission's in-house science service

**www.jrc.ec.europa.eu**


*Serving society*
*Stimulating innovation*
*Supporting legislation*

# Radiation damage in nuclear ceramics

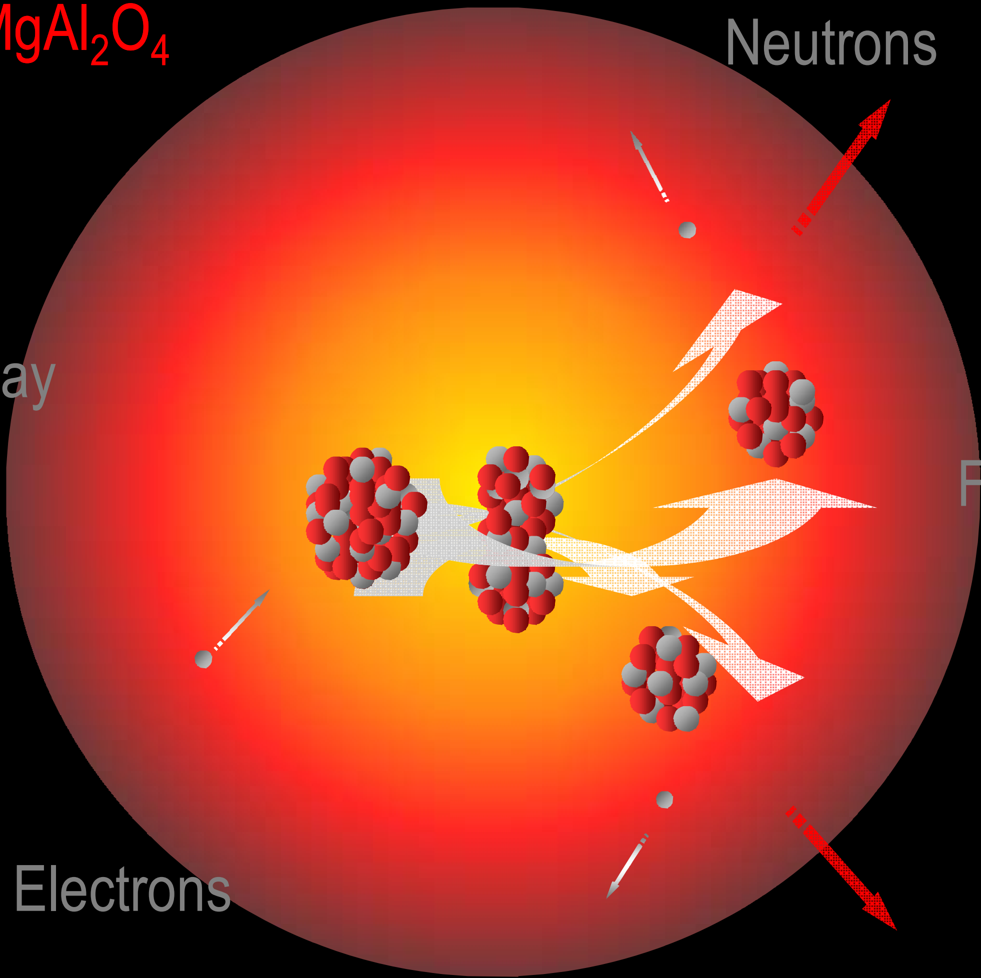

Commission européenne

# The JRC - ITU

## 7 Institutes in 5 Member States **(4 with nuclear activities)**

**IRMM** - *Geel, Belgium*
Institute for Reference Materials and Measurements

**ITU** - *Karlsruhe, Germany*
Institute for Transuranium Elements

**IE** - *Petten, The Netherlands – Ispra, Italy*
Institute for Energy

**IPSC** - *Ispra, Italy*
Institute for the Protection and Security of the Citizen

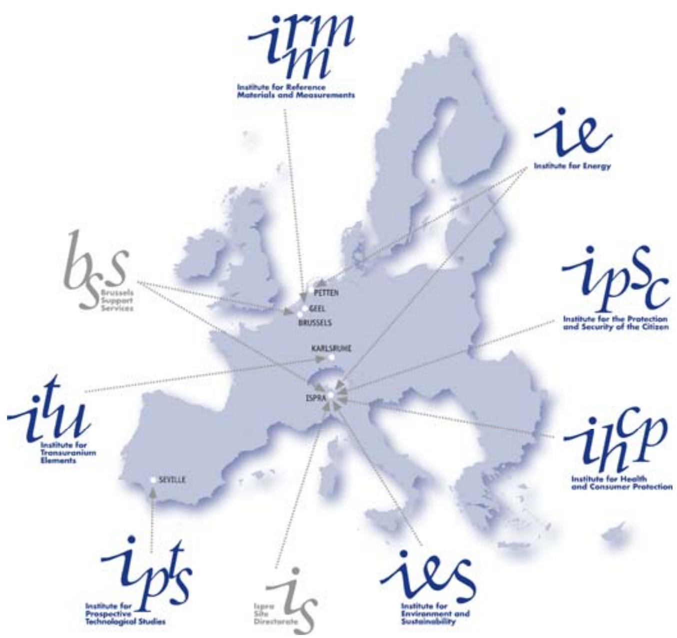


**Governance:**

**Board of Governors (Member States)**

**EU parliament (Framework Programme, budget)**

**~ 2750 staff**
**~ 330 M€/y budget (+ 40 M€/y competitive income)**

# Rationale

- Lifetime of nuclear materials is reduced due to radiation damage build-up.
- Most properties (thermo-physical, mechanical, chemical) are affected by radiation damage (normal and accidental conditions).
- An accurate understanding of the mechanisms of damage production and annealing should help to forecast the behaviour of a given material exposed to different sources of damage.
- Design the materials that will resist to radiation damage.

# Damage along the fuel cycle

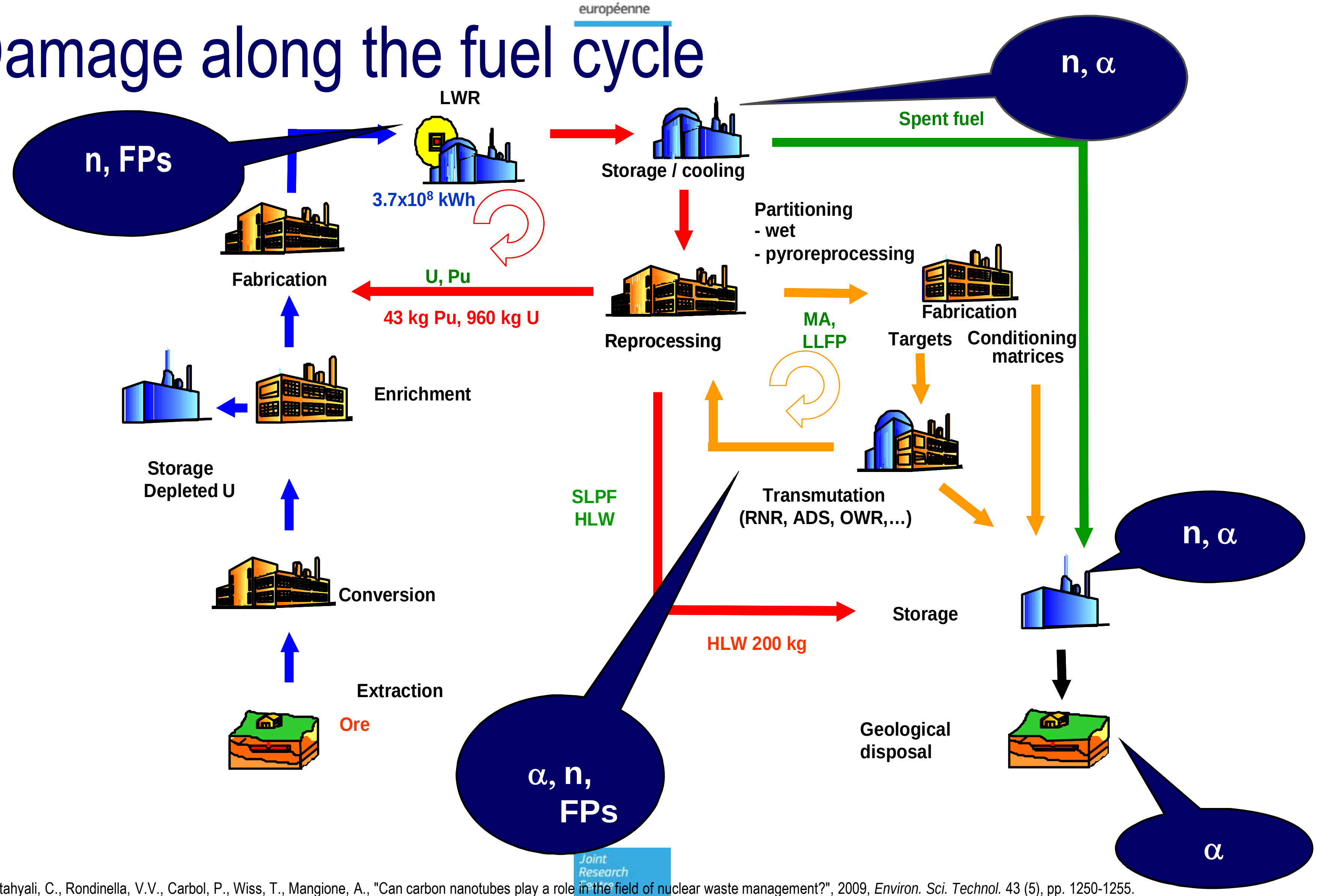


Belloni, F., Kütahyali, C., Rondinella, V.V., Carbol, P., Wiss, T., Mangione, A., "Can carbon nanotubes play a role in the field of nuclear waste management?", 2009, *Environ. Sci. Technol.* 43 (5), pp. 1250-1255.

# Content

Commission européenne

Methodology – Basic processes

Examples

- High burnup $UO_2$ fuel
- Spent fuel (alpha-doped $UO_2$)
- Spinel $MgAl_2O_4$ (transmutation matrix)
- Waste conditioning matrices ($CaZrTi_2O_7$)

Conclusions

# Materials considered

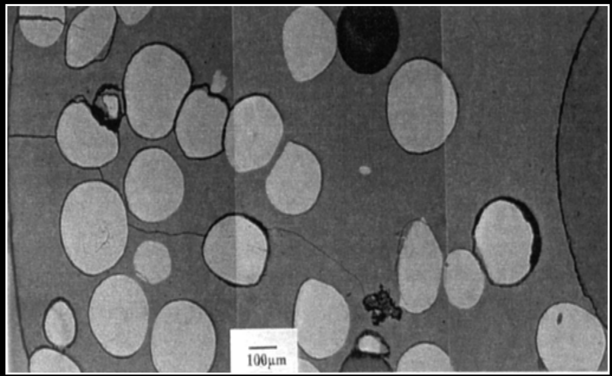


Transmutation targets - IMF

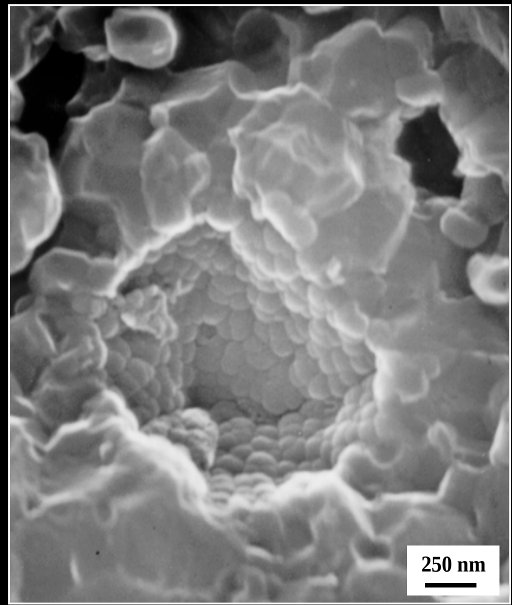


Nuclear fuels

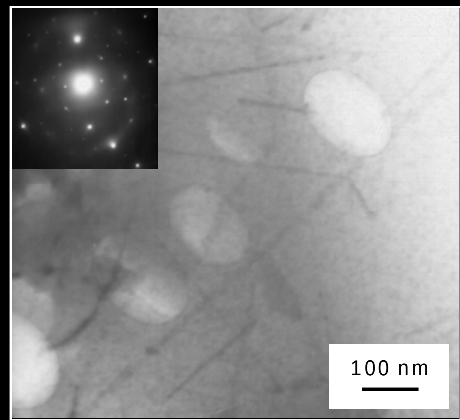


Waste matrices

# Methodology

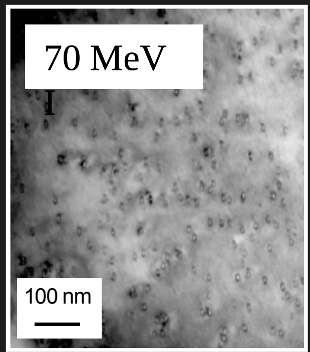


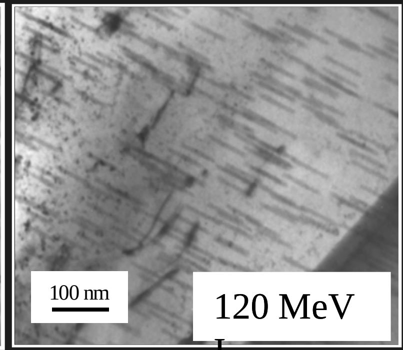


$CeO_2$ $Nd_2Zr_2O_7$

Single effect studies: irradiation with selected ions at given energies, fluences, T^ures^


$(U,^{238}Pu)O_2$

Doping with alpha-emitters for homogeneous damage and helium distribution

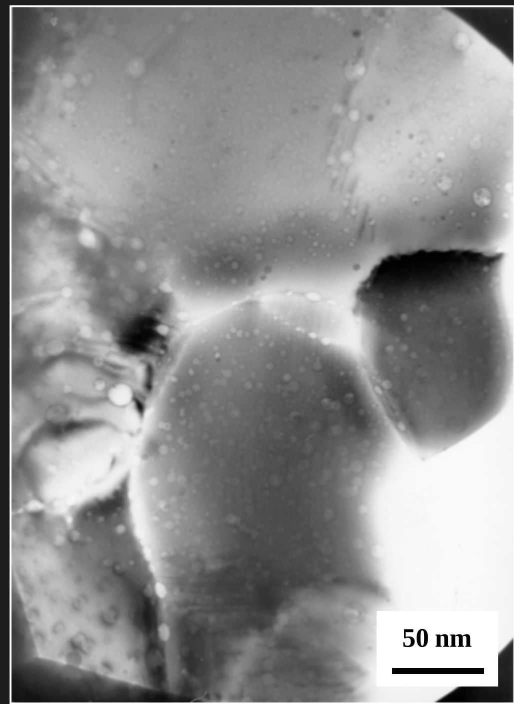


$UO_2$ - 75 $GWd/t_U$

Concomittant effects of different damage sources

# Methodology

Commission européenne

**Irradiated fuels, alpha-doped material, implanted samples**

**Property changes vs. $\alpha$-damage (time)**

**Radiation damage mechanisms**

**radiation damage**

**gas accumulation**

**oxidation**

**He accumulation/ release behaviour**

**Annealing behaviour**

**Swelling, hardness, thermal diffusivity, oxygen potential**

**defects, dislocation loops, He bubbles, internal stress**

**Tools: SEM-TEM, XRD, DSC, Laser Flash, KC, Hardness Meas.**

Joint Research Centre

# Interaction of a charged particle with matter

Inelastic collisions with an electron

main process of energy loss producing excitation and ionization

Inelastic collisions with a nucleus

Bremsstrahlung and coulombic excitation

Elastic collisions with a nucleus

Rutherford diffusion

Elastic collisions with an electron

# Some pioneers….



"Les rayons alpha sont des projectiles matériels susceptibles de perdre de leur vitesse en traversant la matière" (1900)

H. Becquerel

P. Curie

M. Curie-Slodowska

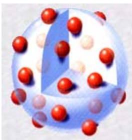

E. Rutherford

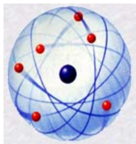

N. Bohr

E. Fermi

E. Schrödinger

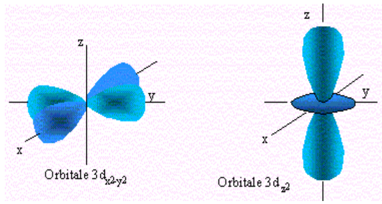


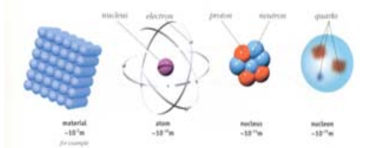

1896 — 1911 — today….

# Range of different particles

Commission européenne

| | Energy, keV | Range, µm | dE/dx, Nucl./Elec. | Defects formed |
|---|---|---|---|---|
| Light FPs | 95000 | 9 | 0.03/0.97 | 40000 |
| Heavy FPs | 67000 | 7 | 0.06/0.94 | 60000 |
| $\alpha$-particles | 5000 | 12 | 0.01/0.99 | 200 |
| Recoil nucleus | 95 | 0.02 | 0.90/0.10 | 1500 |
| Cosmic rays ($p^+$) | $10^{17}$<br>$10^{6}$ (typical) | Light years ! | | |

# Damage in $UO_2$

Cascade from a recoil (SRIM2000)

$Ed_O = 20$ eV

$Ed_U = 40$ eV

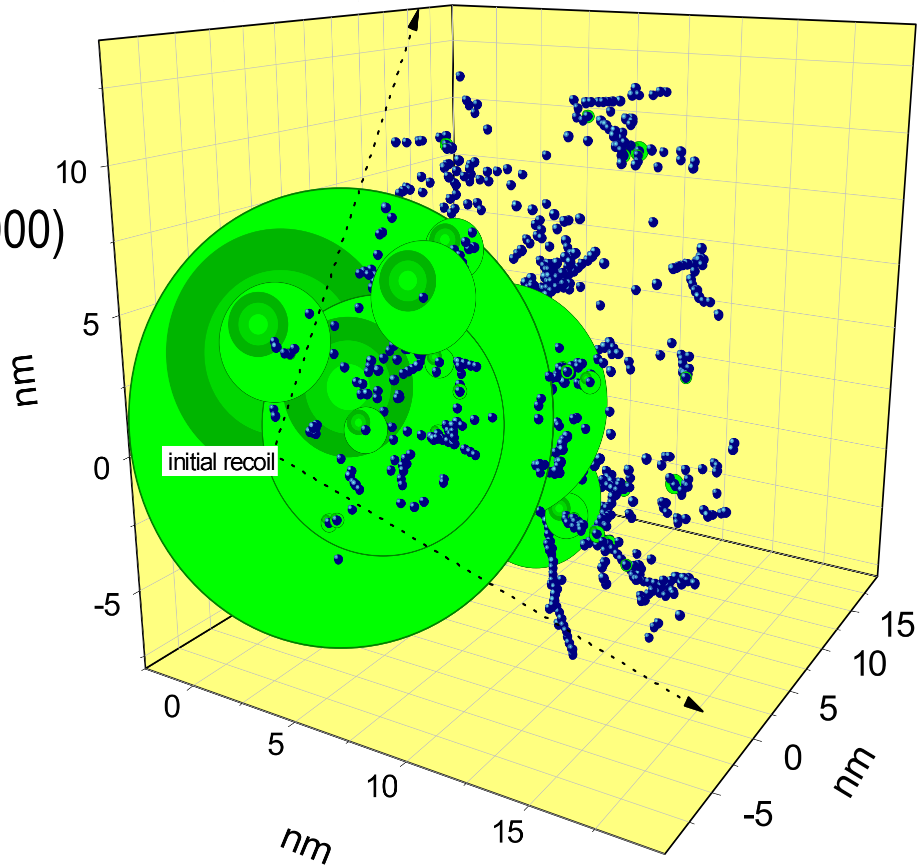


typical pka energy ~ 50 eV; only a few > 2 keV

Ziegler, J. F., Biersack, J.P., Littmark, U., The Stopping and Range of Ions in Solids, Pergamon Press, Oxford, 1985

# Nuclear fission

Commission européenne

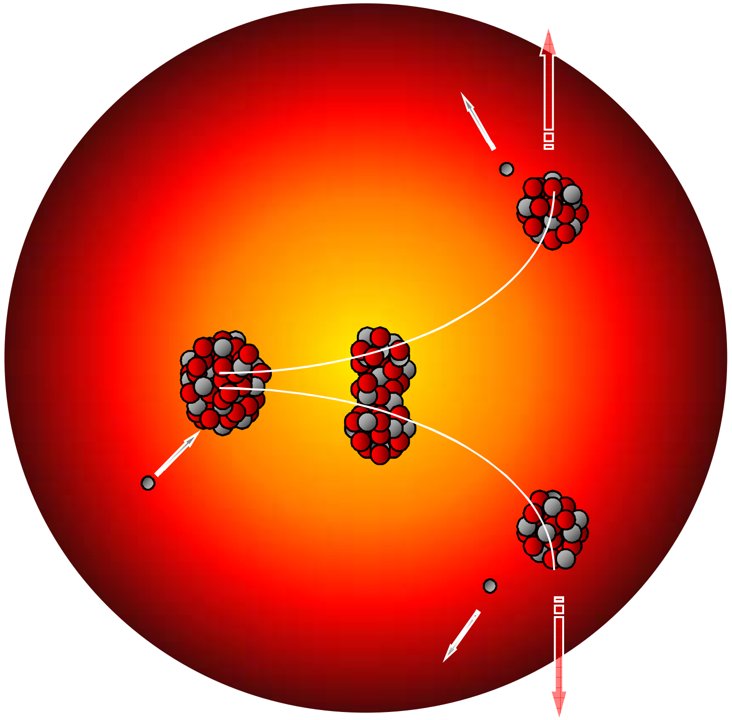

Only the electrons which "rotate" at a higher speed than that of the fission fragment are carried away.

Fission rate:

10 $f \cdot \mu m^{-3} s^{-1}$ ...$10^9$ $f \cdot \mu m^{-3}$ in 3 years

(~$7 \cdot 10^{10}$ atoms$\cdot \mu m^{-3}$ in $UO_2$).

Displacements:

two fission fragments ( 67 and 95 MeV) produce ~$10^5$ displacements along 7-9 $\mu$m range.

→ **~1 dpa / day**

At the end of irradiation each fuel atom has been displaced a few thousand times!

Joint Research Centre

# Track formation in $UO_2$ by swift heavy ions

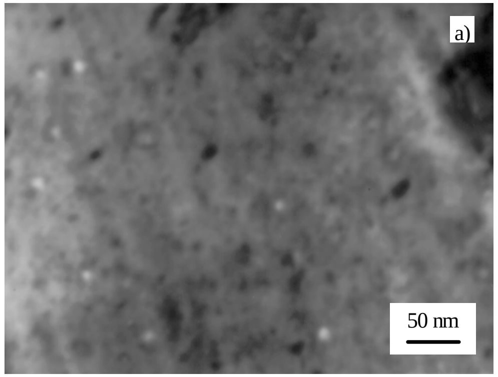


a) 1300 MeV $^{238}U$
dE/dx = 56 keV/nm

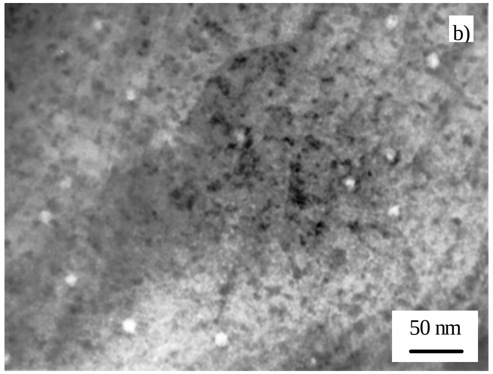


**b) 2713 MeV $^{238}U$ dE/dx = 59 keV/nm**

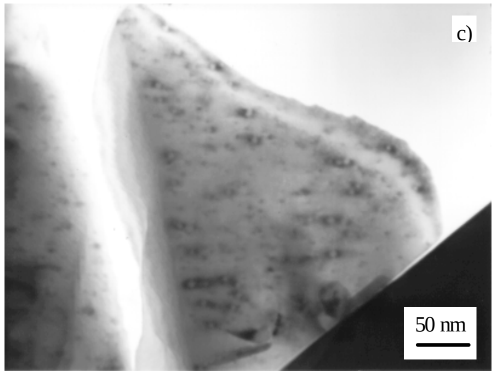


c) 173 MeV Xe
dE/dx = 29 keV/nm

Ion tracks observed by TEM

Thermal spike effect (*Toulemonde* model)

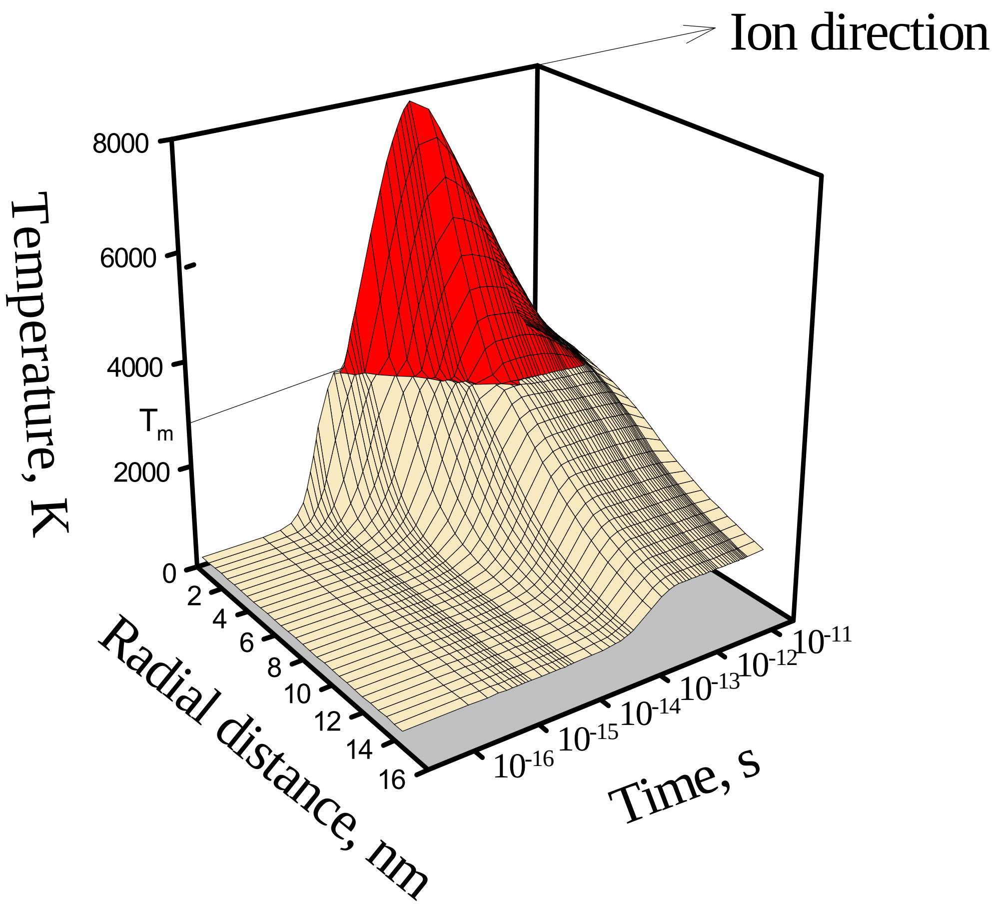


Radial temperature spread in the track
Here corresponding to the case b)
i.e. maximum energy 2.7 GeV

# Thermal spike effects in $UO_2$

Commission européenne

Track formation at $UO_2$ surface [1] and fission-spike induced phase change in $U_4O_9$ needles existing in $UO_{2+x}$ (at T > 1150° C [2]).

Fission-enhanced diffusion of U in $UO_2$ (athermal below 1100 ° C) explained by thermal and pressure effects of fission spikes [3].

Re-solution of fission gas bubbles due to passing fission products [4].

Radiation-enhanced creep due to thermal spikes [5].


[1] C. Ronchi, J. Appl. Phys. 44 (1973) 3575.
[2] H. Blank, Phys. Stat. Sol. (a) 10 (1972) 465.
[3] Hj. Matzke, Rad. Effects 75 (1983) 317.
[4] H. Blank and Hj. Matzke, Rad. Effects 17 (1973) 57.
[5] D. Brucklacher and W. Dienst, J. Nucl. Mater. 42 (1972) 285.

# Fission track at the surface of $UO_2$

The spike produces a shock wave (strong compression wave outside the track core) which can result on tensile stresses on the surface layer

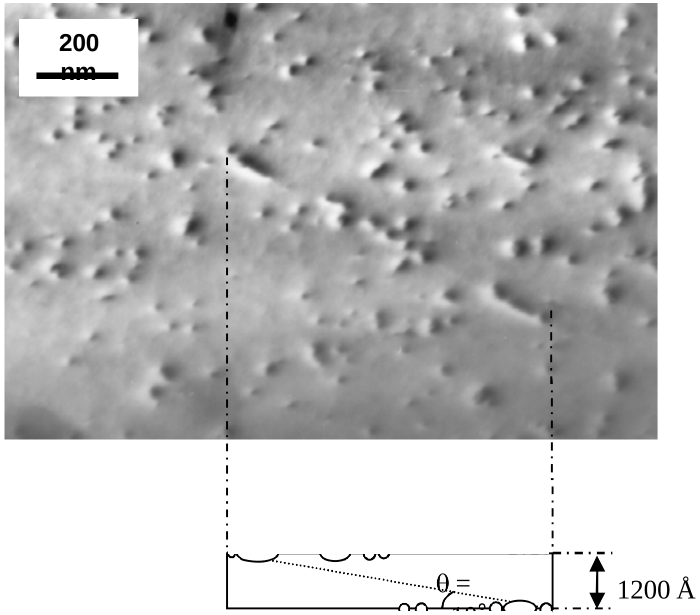


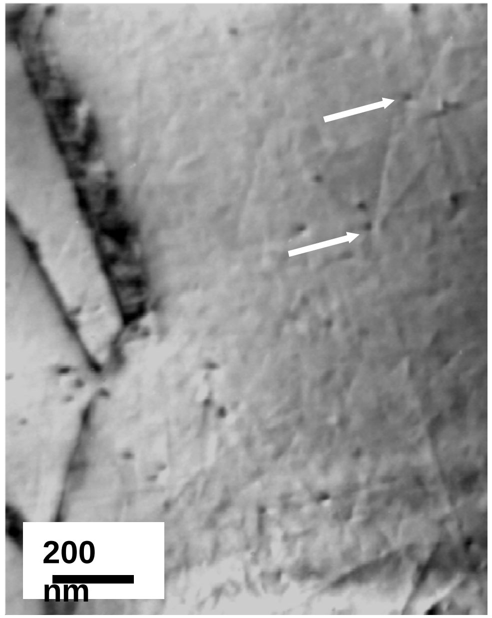


TEM micrograph evidencing the nature of surface tracks, i.e. intermittence of short segments (e.g. two FFs exits indicated by the arrows on the picture right)

# Nuclear Fuel

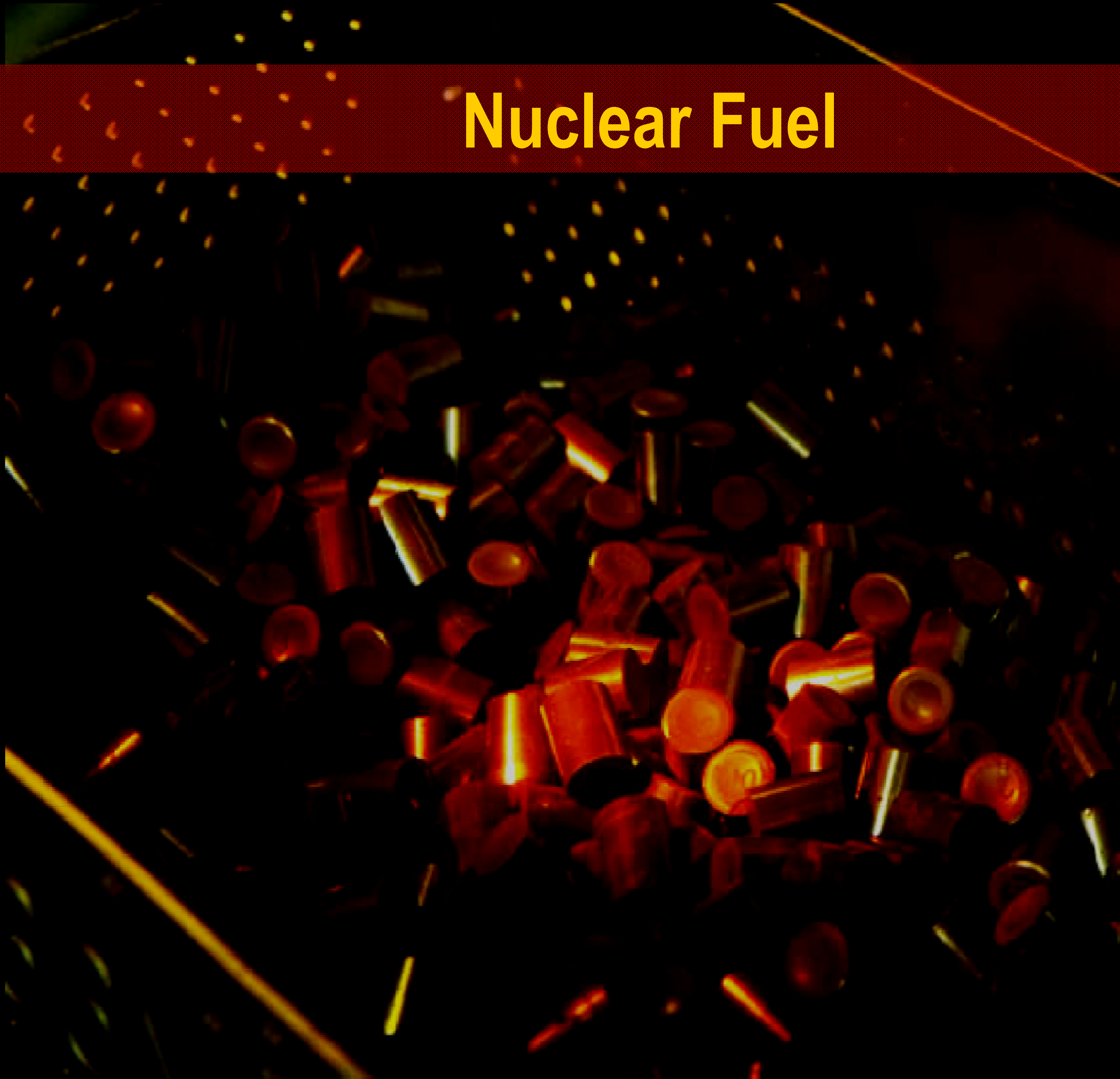

# $UO_2$ - fuel and waste

Commission européenne

400 operating reactors worldwide producing a large stockpile of radioactive waste. In the past decade 300000 Tons of spent fuel, 1% of Pu (3000 tons), 0.1% MA, (300 tons), and 400 tons of LLFPs.

Increase of the burnup (55 $GW_d/t_U$).

Spent Fuel Stability (public acceptance).

Two major visions:

- consider the SNF as ultimate waste.
- take benefit from the fissile material still present in the SFN and isolate the fission products and minor actinides in waste forms (implies reprocessing).

Basic questions on the radiation stability of $UO_2$ (HBS, disposal).

# Safety of nuclear fuels



We do not want high burnup LWR fuel to cause rod failure:

- no excessive pushing of clad.
- no excessive fission gas release hence rod pressurization.
- no fuel melting.

We want to predict the effects of burnup and irradiation temperature on in-pile behaviour (e.g. thermal conductivity, structural stability) but also on the long term behaviour (storage).

# Re-solution of bubbles - densification

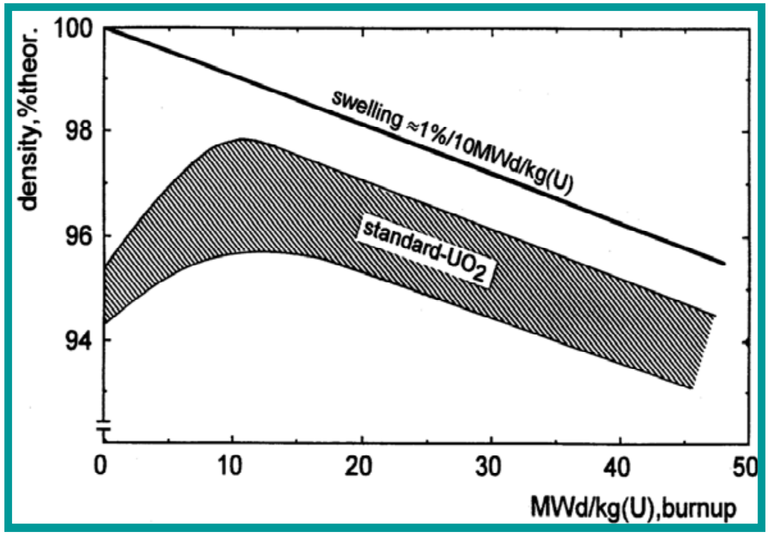


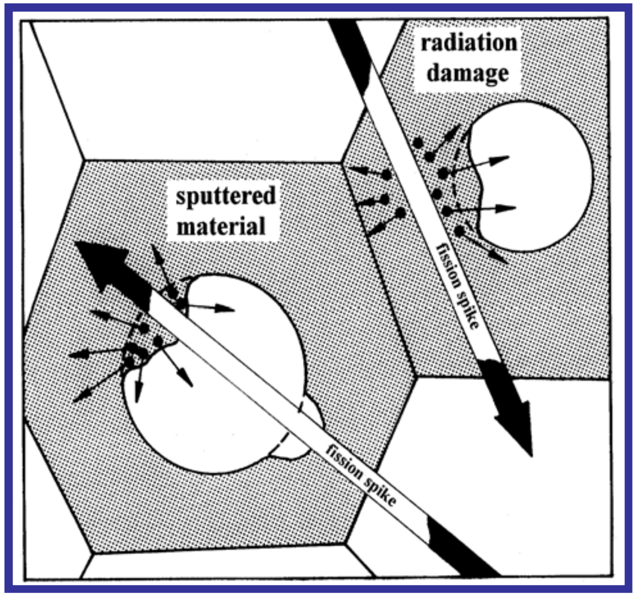


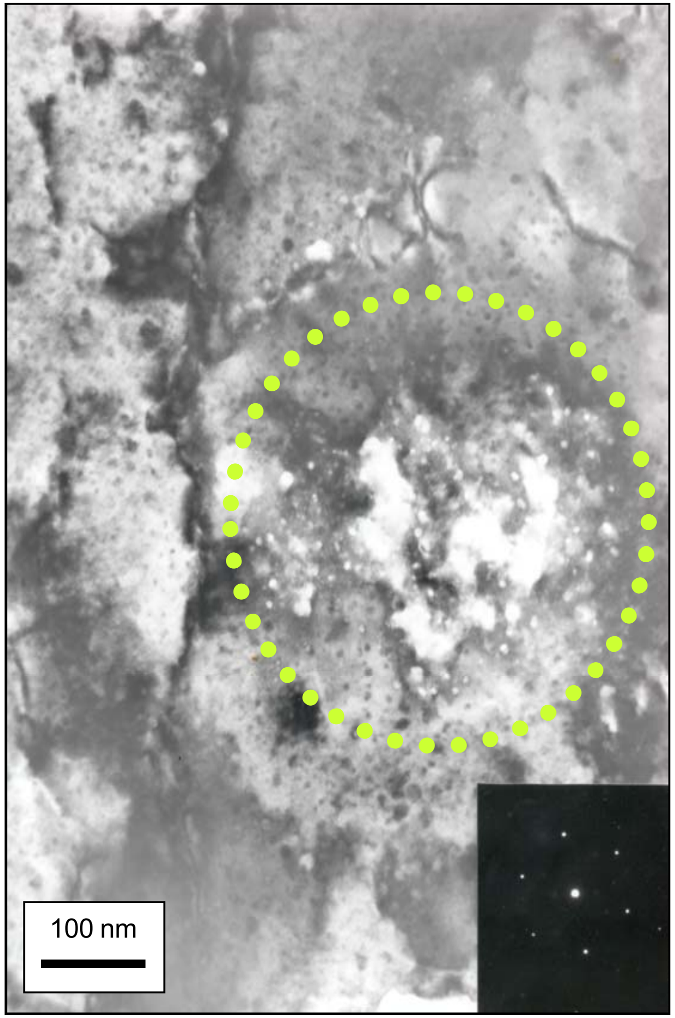


Ronchi, C., Wiss, T., Fission-fragment spikes in uranium dioxide, 2002, Journal of Applied Physics 92 (10), pp. 5837-5848

# Effect of burnup, $T_{irr}$

## Thermal diffusivity of $UO_2$; $\lambda = (A + BT)^{-1}$

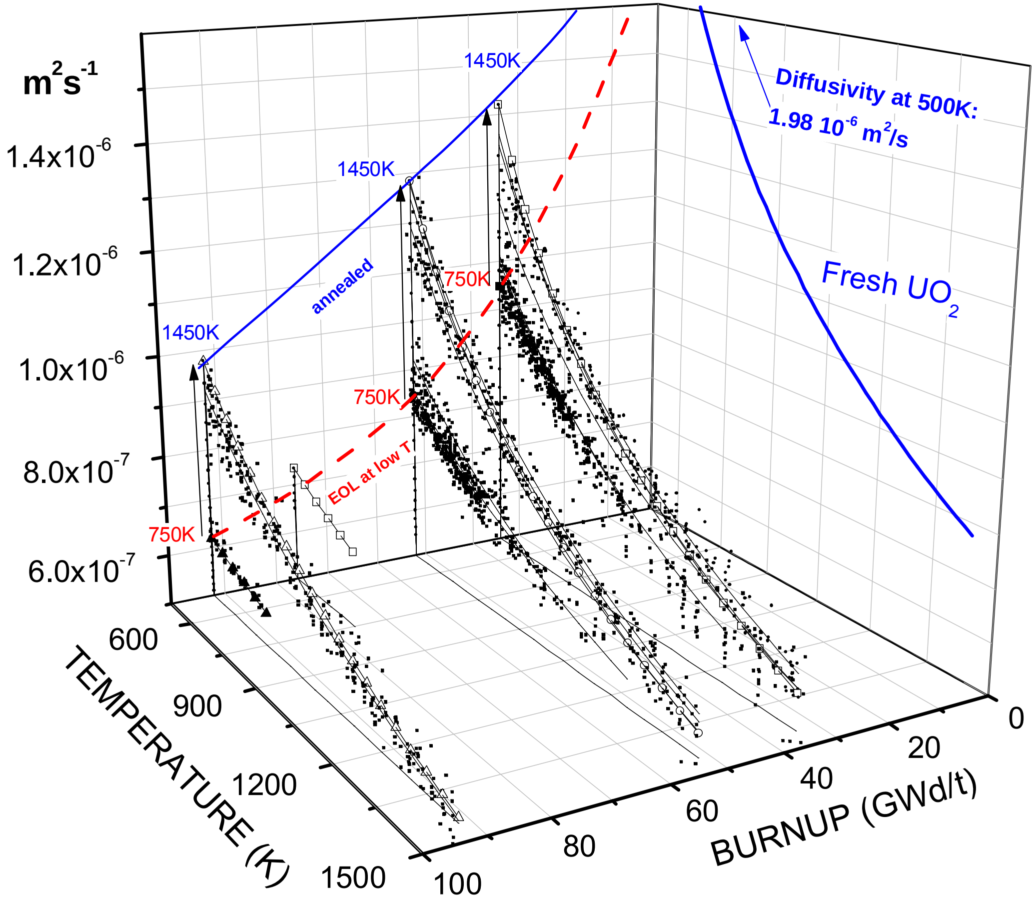


HBRP experimental database
4 burnup x 4 $T_{irr}$

High burnup fuel samples typically failed at $T \geq T_{irr}$. Annealing could be measured through thermal cycling only for high $T_{irr}$ fuel.

Joint Research Centre

# $\lambda = (A + BT)^{-1}$

Commission européenne

***A*** **accounts for phonon-impurity scattering due to:**

- **soluble fission products** *(dependent on burnup only)*
- **point defects** *(dependent on temperature, saturated at low burnup)*
- **dynamically dissolved *FG* and volatile *FP*** *(dependent on burnup and temperature)*

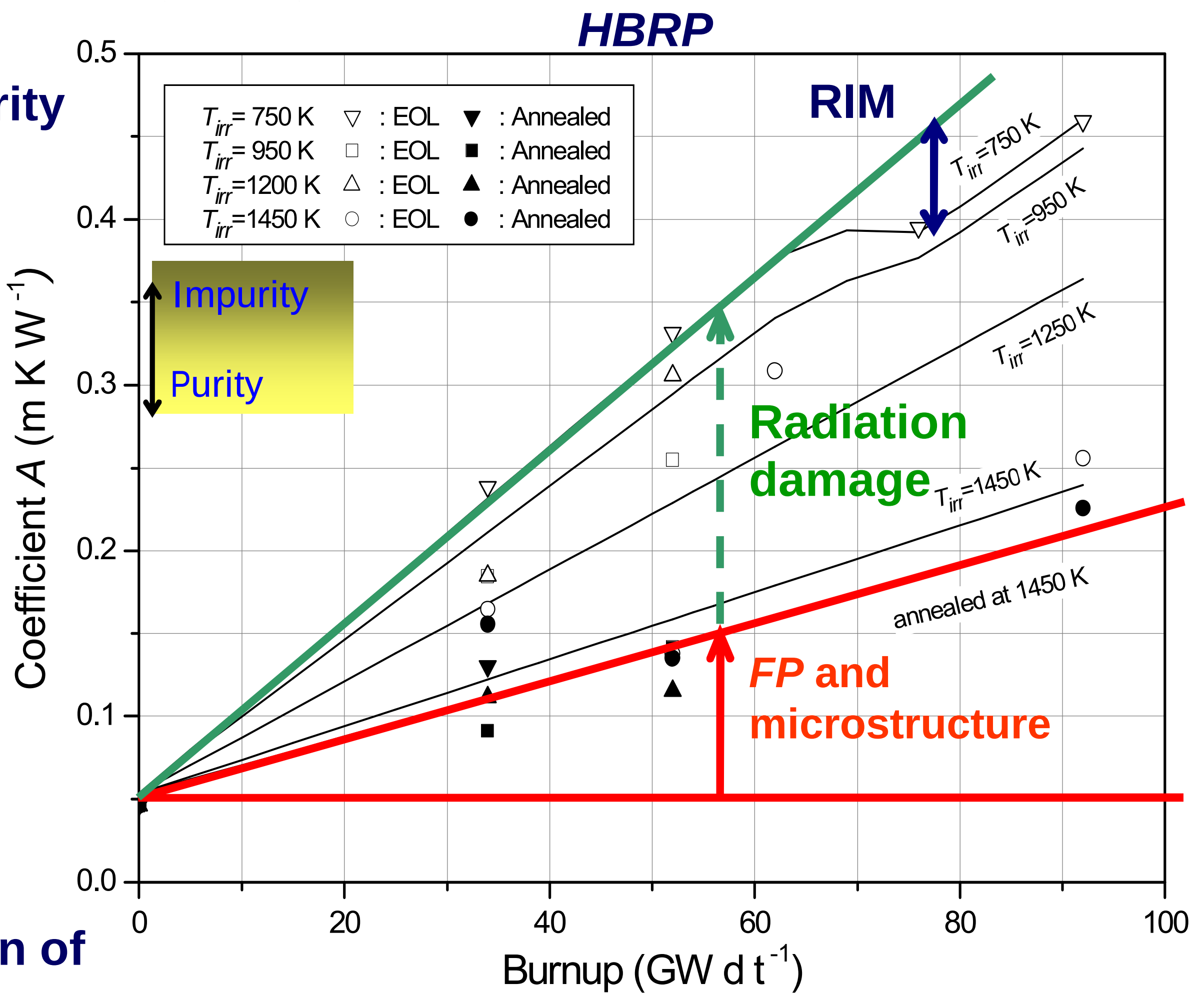


***B*** **should account for variation of elastic properties with burnup:**

- presently based on empirical fitting

**effect of thermal annealing: decrease of *A* and increase of *B***

Joint Research Centre

# Application to commercial $UO_2$

Commission européenne

## 100 GWd/t

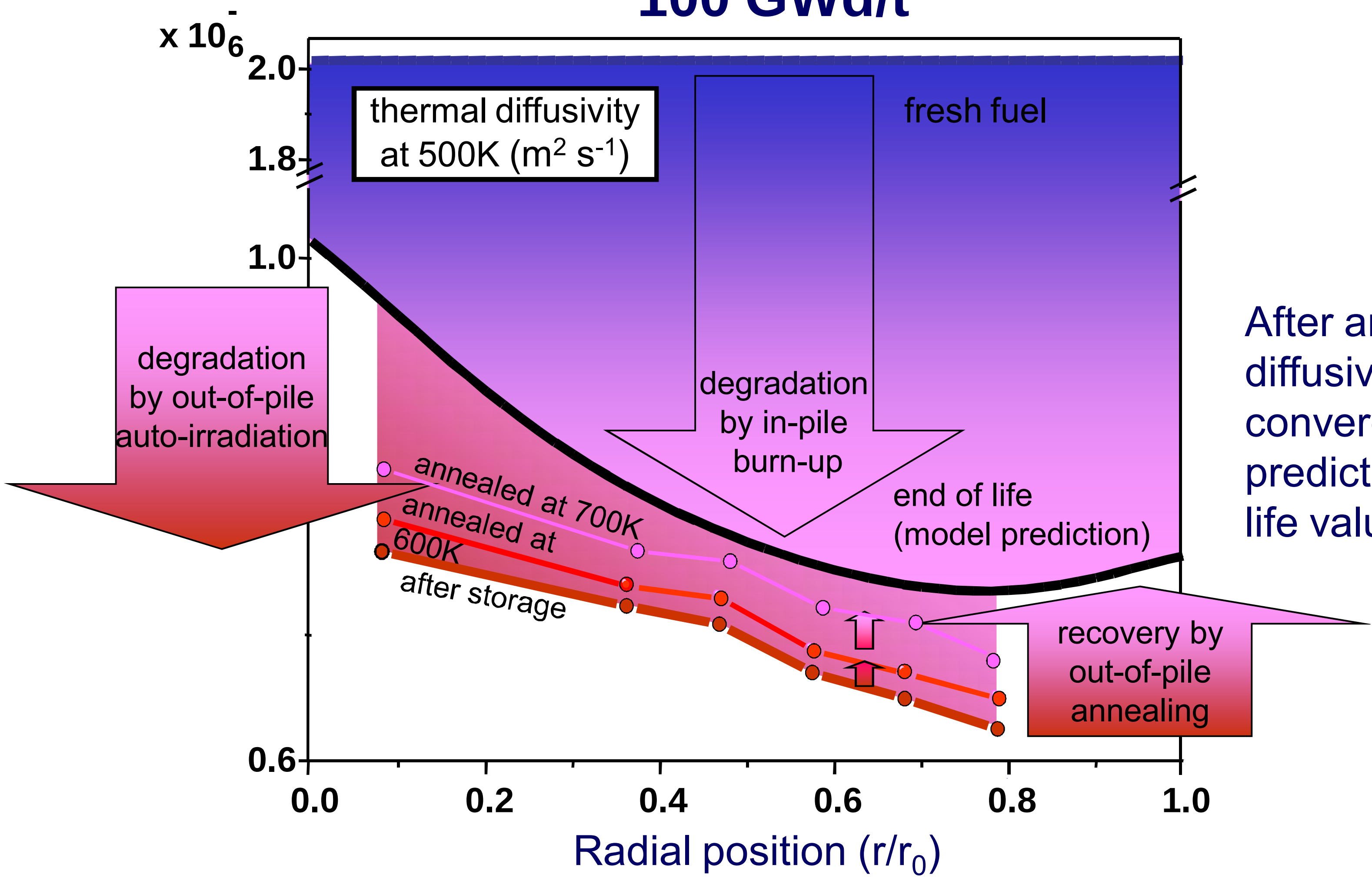


After annealing, diffusivity converges to predicted end-of-life values.

# Spent fuel

# Evolution of spent fuel

Commission européenne

- Assessment of the evolution of spent fuel prior to water access …description of the initial condition of spent fuel that is intended for disposal in a geologic repository.

- What will be the structure after cumulating alpha-decay ? Emphasis will be … on the evolution of the microstructural stability of spent fuel (waste matrices) as a function of time.

- The final aim is to extrapolate experimentally but also to model measured effects to the storage times relevant for the applications of interest (interim storage, final disposal).

# Aging of nuclear fuels

Commission européenne

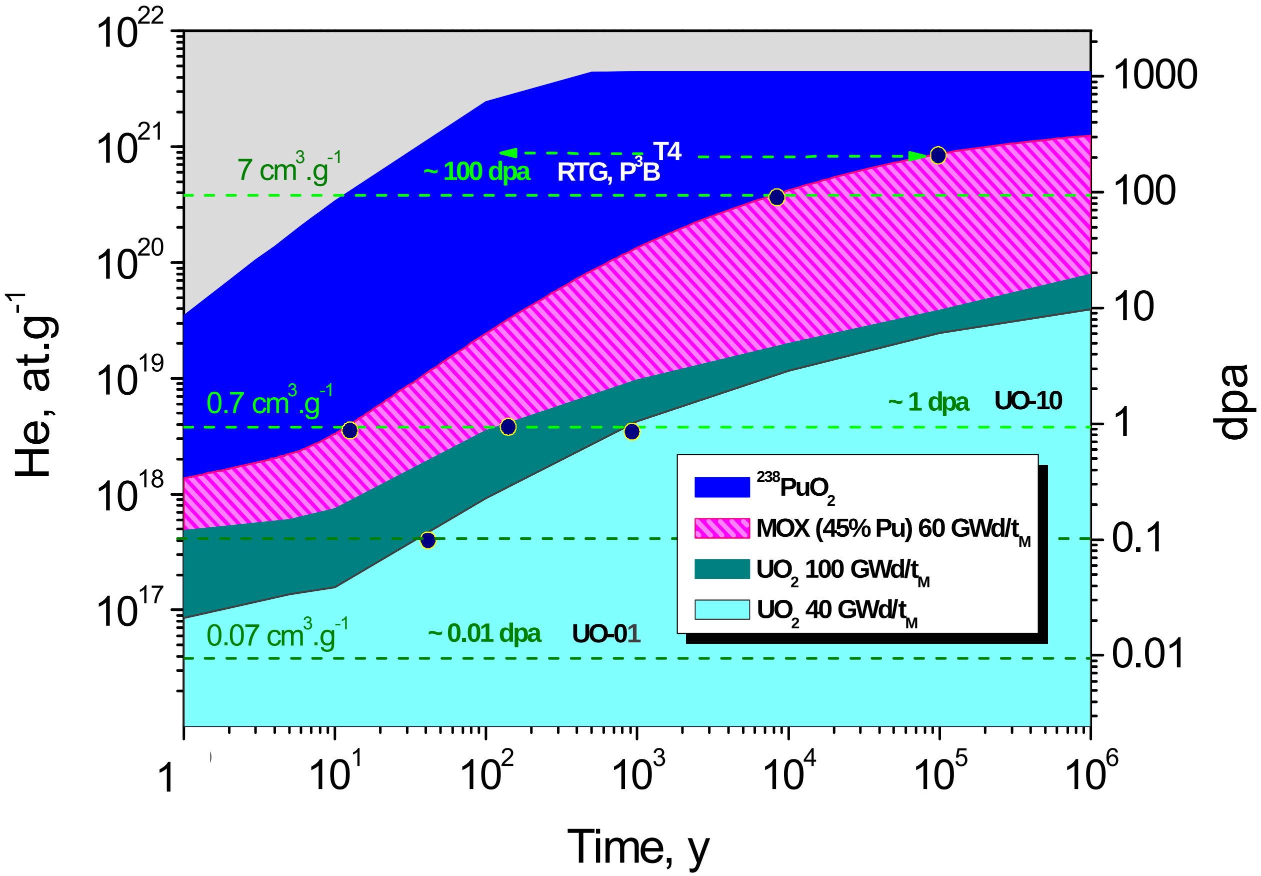


Free volume in a rod: 20 cm$^3$

Pressure at EOI: 40 bar

Hydrostatic P disposal: 50 bar

Increase e.g. 50 bar

- RTG = MOX 8000 y

Displacements per atom

Cascades during alpha-decay

Elastic – inelastic effects

Annealing

Structural integrity

**Keywords**: solubility, diffusion coefficient, He-release, swelling, fracture, source term (S/V)

Centre

# TEM alpha-damaged $(U_x,Pu_{1-x})O_2$

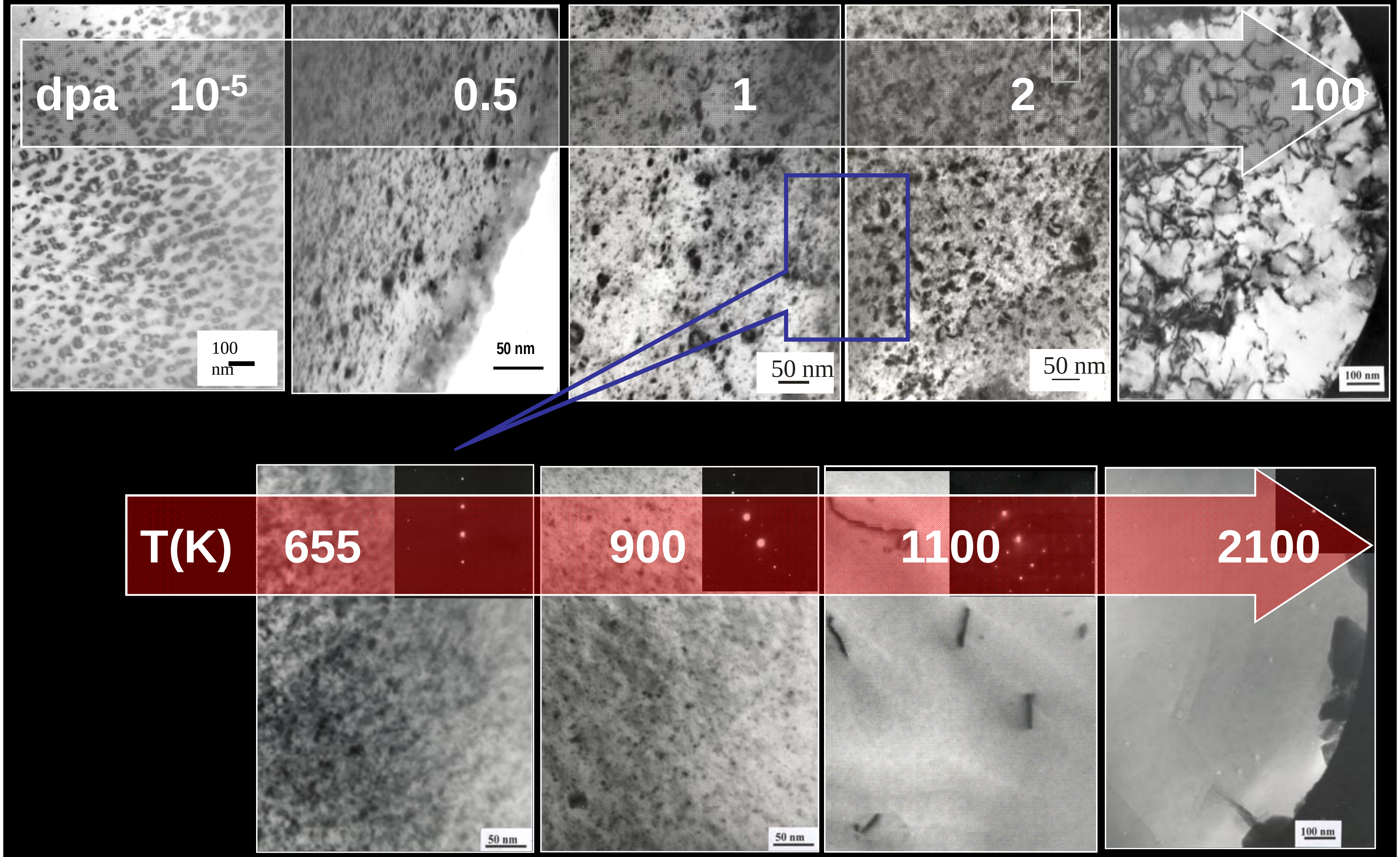

# XRD analysis of α-damaged samples

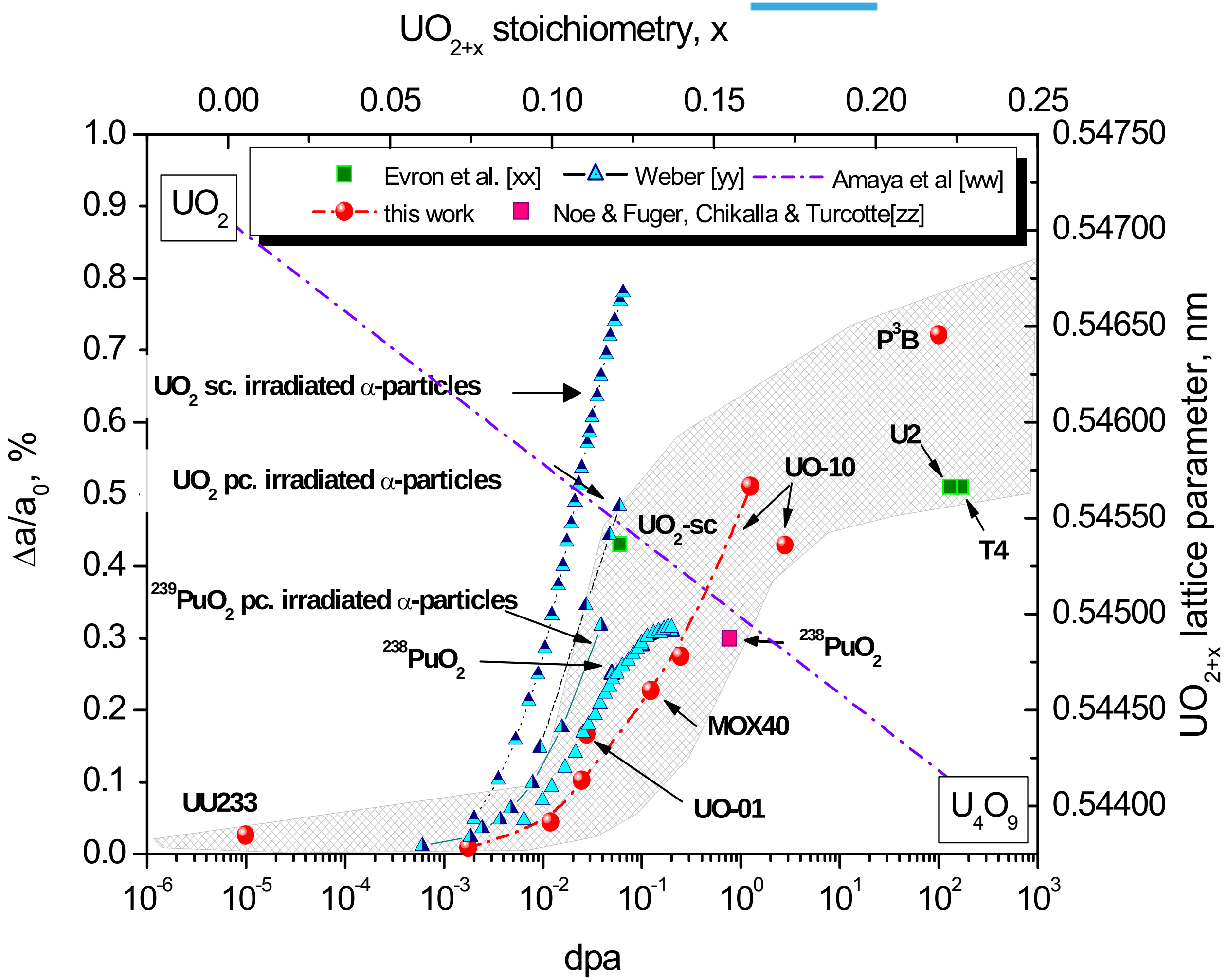


- Oxydation a↓
- Damage a↑
- Kinetic effects
- Saturation

To be submitted as "From curium heat generator to urano-thorianite minerals as analogues of old nuclear waste",

by T. WISS, J.-P. HIERNAUT, D. ROUDIL, J.-Y. COLLE, H. THIELE, R. JARDIN, E. MAUGERI, V. RONDINELLA, R. KONINGS, Hj. MATZKE, W. WEBER

# Apparent specific heat during annealing

Commission européenne

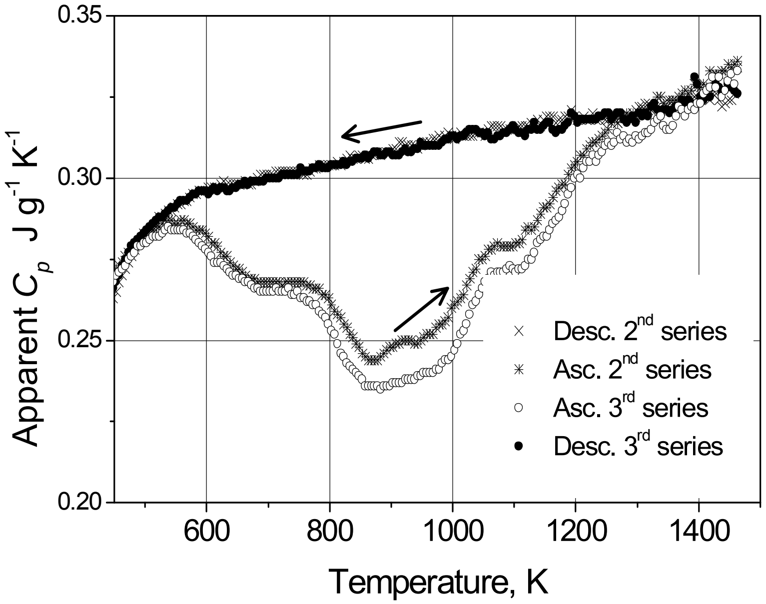


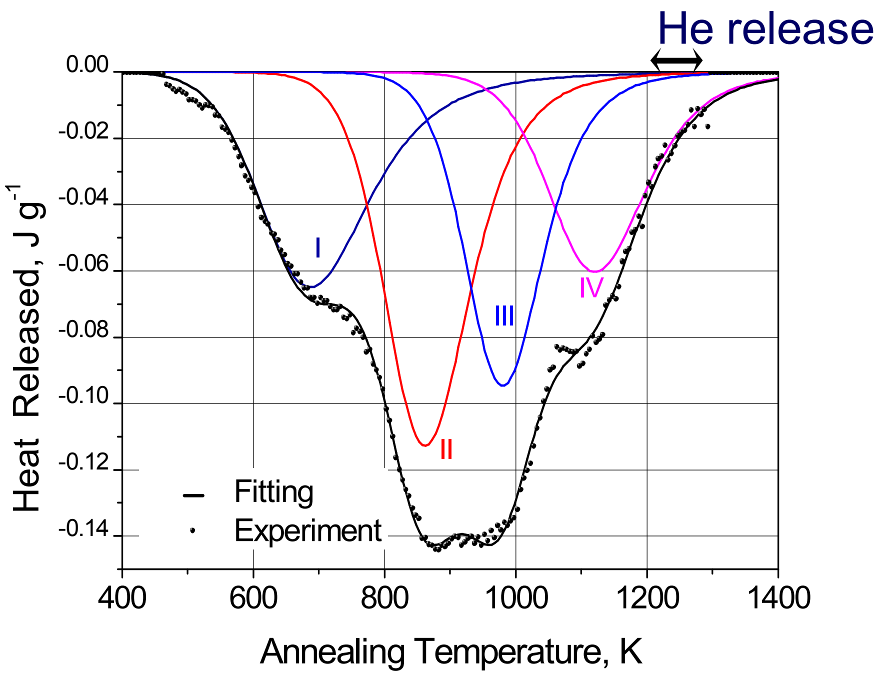


Reproducible runs after 5 and 6 months storage (15 K min$^{-1}$).
The deviation of initial $C_p*(T)$ from annealed $C_p(T)$ is due to recovery of latent heat of lattice defects.
Curves corrected for the $\alpha$-decay heat (~0.14 Jg$^{-1}$K$^{-1}$)

Heat effects

I : O vacancy-interstitial recombination (14 J/g)

II : U vacancy-interstitial recombination (19 J/g)

III : Loop annealing (12 J/g)

IV : Void precipitation (15 J/g)

Joint Research Centre

# DSC results

Commission européenne

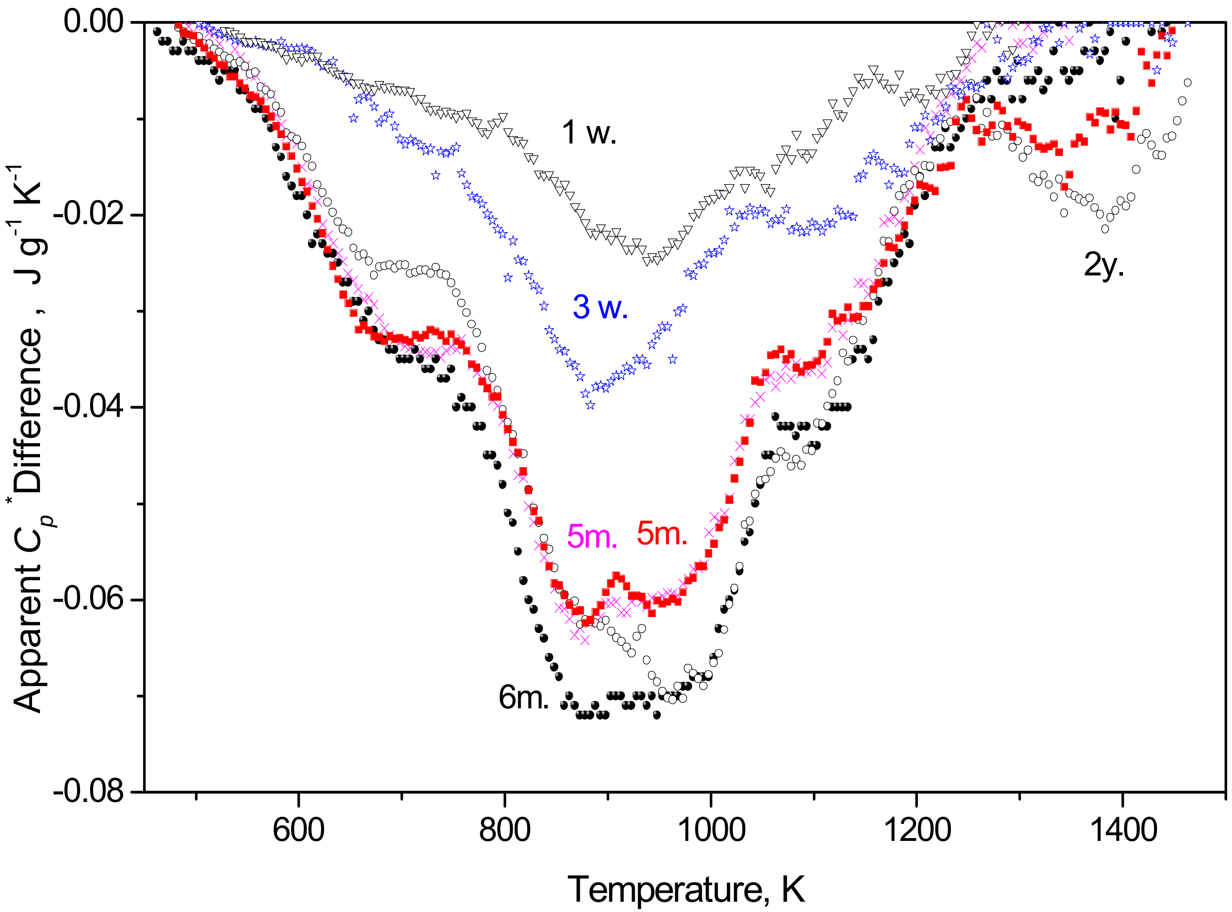


Joint Research Centre

# Defects formation

Commission européenne

Annealing of defects produces measurable heat. Four distinct annealing stages were observed whose analysis was made possible by a comparative analysis with the independent recovery processes of **lattice parameter, thermal diffusivity, void/dislocation growth and $\alpha$-helium release.**

Defect Concentrations and Enthalpies Measured in the Four Recovery Stages

| *Stage* | I | II | III | IV |
|---|---|---|---|---|
| Total released energy | 14.7 J $g^{-1}$ | 19.6 J $g^{-1}$ | 11.8 J $g^{-1}$ | 15.0 J $g^{-1}$ |
| Mechanism | O vacancy-interstitial recombination | U vacancy-interstitial recombination | Loop formation | Void precipitation |
| Defects involved in recombination | $2.4\ 10^{20}$ $cm^{-3}$ | | - | - |
| Defects involved in precipitation | - | - | $7.0\ 10^{19}$ $cm^{-3}$ | |
| Diffusion Enthalpy, *H* | 0.62 eV | 1.34 eV | 2.0 eV | 2.0 eV |
| Recovered Energy, *E* | 3.8 ± 0.5 eV | 5.1 eV | 10.6 eV | 13.4 eV |

The $\alpha$-Helium Inventory is $4.4\ 10^{18}$ atoms $cm^{-3}$ , much lower than the defects concentration. Helium released at the end of stage IV is a consequence of defect restructuring but plays no major role in it.

Joint Research Centre

# Evolution of the heat released with storage

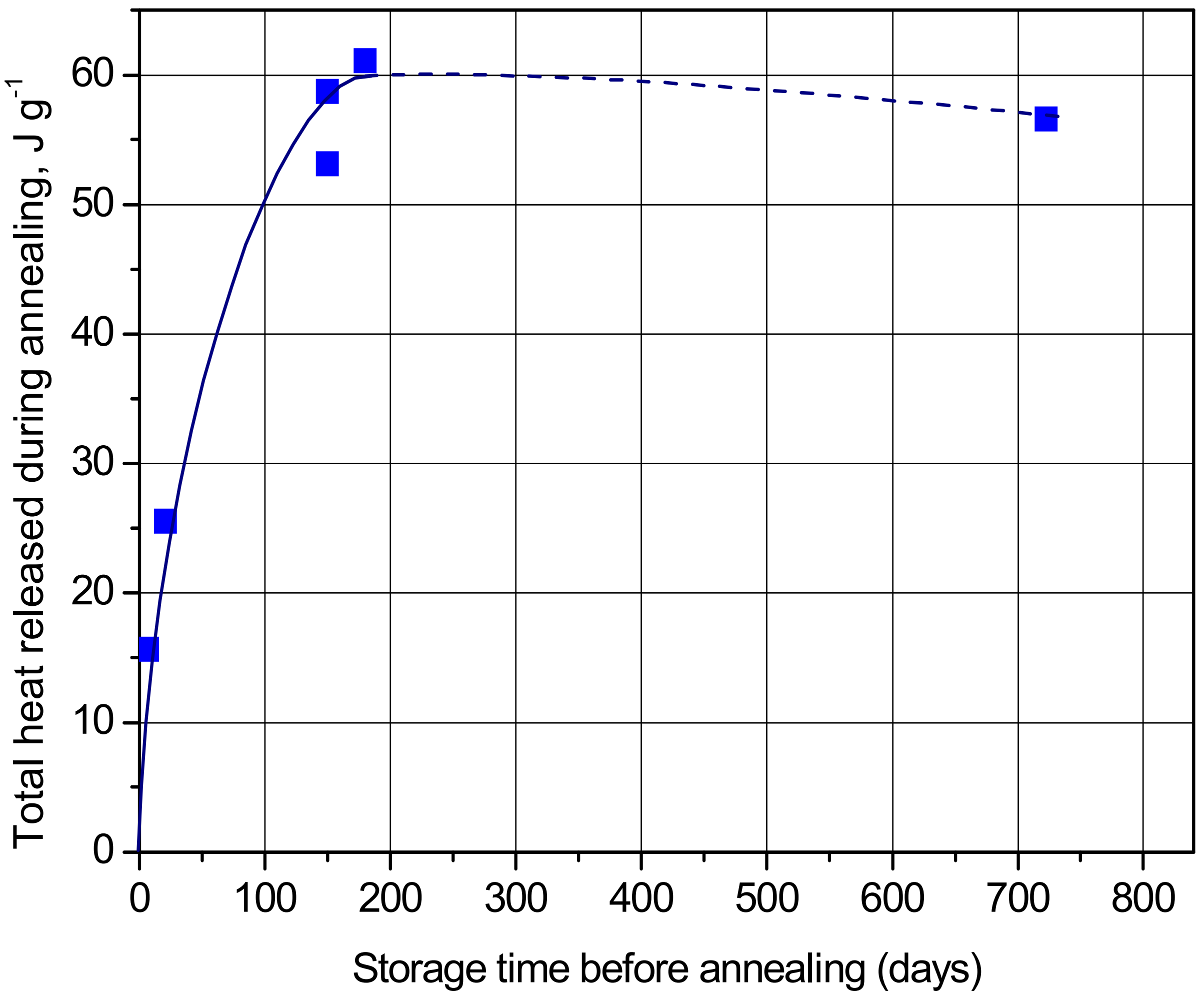

# Alpha-damage in $UO_2$

Commission européenne

- The overall microstructure of alpha-damaged $UO_2$ consists of the rapid formation of dislocation loops. Their growing slows down by re-solution of interstitials…
- …But coalescence of diffusing interstitial-type dislocation loops.
- Rapid lattice swelling and saturation at ~ 2%

  - consequence of extended defects ingrowth (polygonisation?)
- MD studies of prismatic dislocation loops show that interstitial loops can diffuse along the direction of the Burger's vector without an applied stress (B.D. Wirth, Science, 318 (2007) pp 923-924, K. Arakawa, K. Ono, M. Isshiki, K. Mimura, M. Uchikoshi, H. Mori, Science 318 (2007) pp 957-959)

METALS

- Formation of dislocation tangles based on the growth and interaction of prismatic dislocation loops (origin of the HBS ?).

# Conclusions

Commission européenne

- Combined analyses allowed quantification of damage and recovery process.

- Accelerated decay accumulation was validated as representative of long-term ageing of high-level waste forms.

- Comparison with irradiated fuels shows that damage effects and recovery processes during thermal annealing occur by similar mechanisms in $\alpha$- and fission-damaged $UO_2$: → <u>towards a unified understanding of radiation damage.</u>

Joint Research Centre

# Inert matrix for transmutation – $MgAl_2O_4$

# Previous results on spinel irradiations

With neutrons

- Good resistance to void formation (fluences up to $2.3 \times 10^{26}$ n/cm$^2$, $E_n$ >0.1 MeV, 1100K). (F. W. Clinard, Jr, G. F. Hurley and L. W. Hobbs, J. Nucl. Mater. 108&109 (1982) 655.)

  and to void swelling (Hj. Matzke Rad. Effects **64** (1982) 3-33.
- Efficient point defect annihilation by interstitial-vacancy recombination (dpa> 50).

  (K. E. Sickafus, A. C. Larson, N. Yu, M. Nastasi, G. W. Hollenberg, F. A. Garner and R. C. Bradt J. Nucl. Mater. **219** (1995) 128-134.)

With low and medium energy heavy ions

- Al and O sublattices disordering ($2 \times 10^{16}$ Xe-ions/cm$^2$, $E_{Xe}$ = 300 keV, RT

  (A. Turos, Hj. Matzke, A. Drigo, A. Sambo and R. Falcone Nucl. Inst. and Meth. B 113 (1996) 261-265.)

- Spinel amorphization at 100 K when irradiated with $10^{16}$ Xe-ions ($E_{Xe}$ = 400 keV)

  (R. Devanathan, K. Sickafus and M. Nastasi J. Nucl. Mater. **232** (1996) 59-64.)
- Step height swelling of 0.8% for spinel irradiated with $10^{17}$ Ar-ions/cm$^2$ ($E_{Ar}$ = 4 MeV, 200 K) (S. J. Zinkle and G. P. Pells J. Nucl. Mater. **253** (1998) 120-132.)

Commission européenne
Research Centre

# Ion implantation of spinel



## With alpha-particles

- Structurally stable against impact of alpha-particle but formation of He-bubbles.

  (R. Fromknecht, J-P. Hiernaut, Hj. Matzke and T. Wiss, Nucl. Instr. Meth. Phys. Res. **B 166 & 167**, pp. 263 - 269, (2000).)

## Swift heavy ions

- amorphization when irradiated at RT with 72 MeV I-ions ($10^{16}$ ions/cm$^2$) and track formation for FPs-ions.

  (S. J. Zinkle, Hj. Matzke and V. A. Skuratov, Mater. Res. Soc., Warrendale, PA, MRS Symp. Proc. **540** (1999) 299 – 302).

- large swelling (starting at $5 \times 10^{13}$ I-ions/cm$^2$, 72 MeV).

  (T. Wiss and Hj. Matzke, Rad. Measurements, **31** (1999) 507 - 514.)

# Swelling of implanted $MgAl_2O_4$

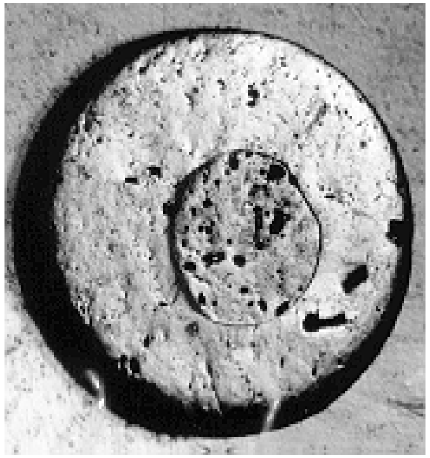

Ions: Iodine

E: 72 MeV

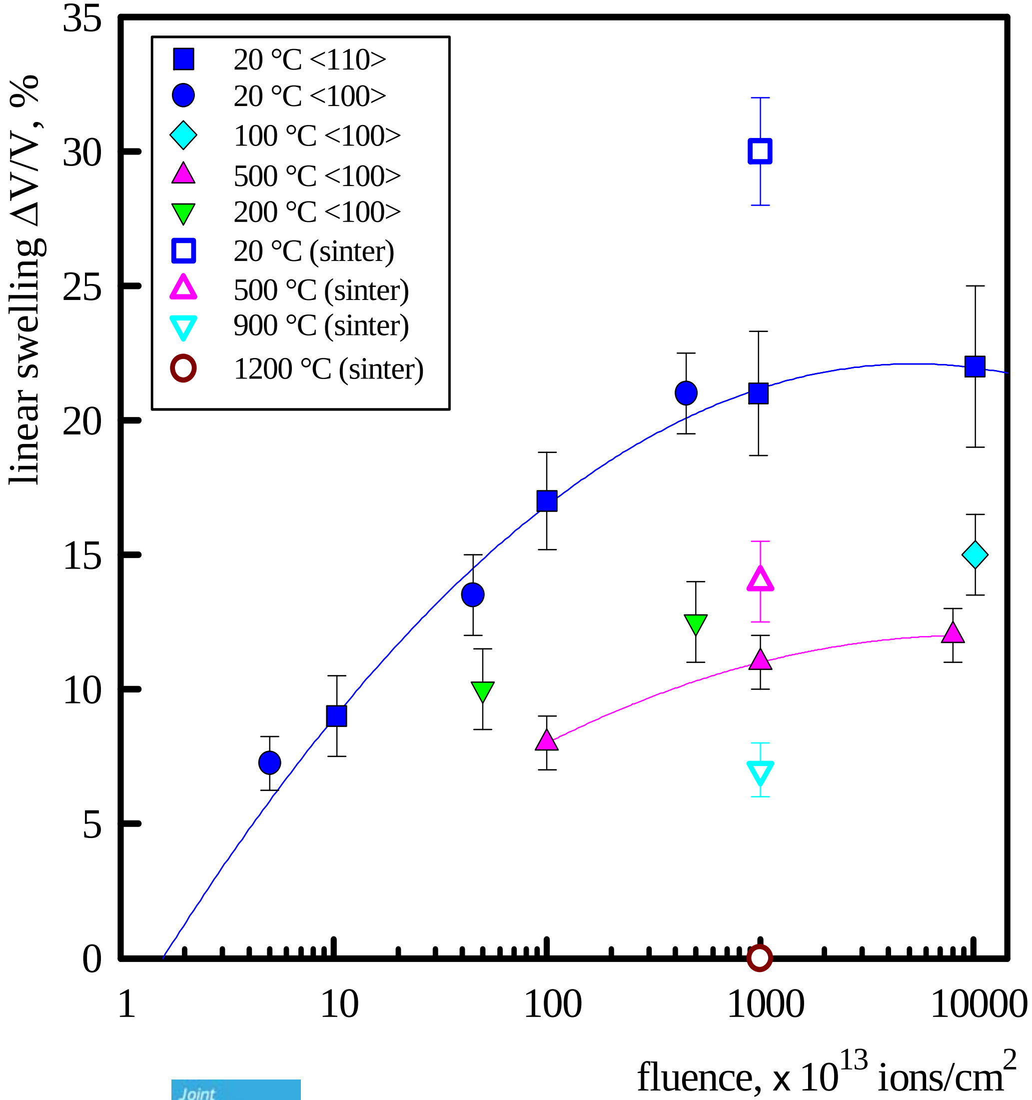


Commission européenne
Joint Research Centre

# TEM of ion tracks in $MgAl_2O_4$

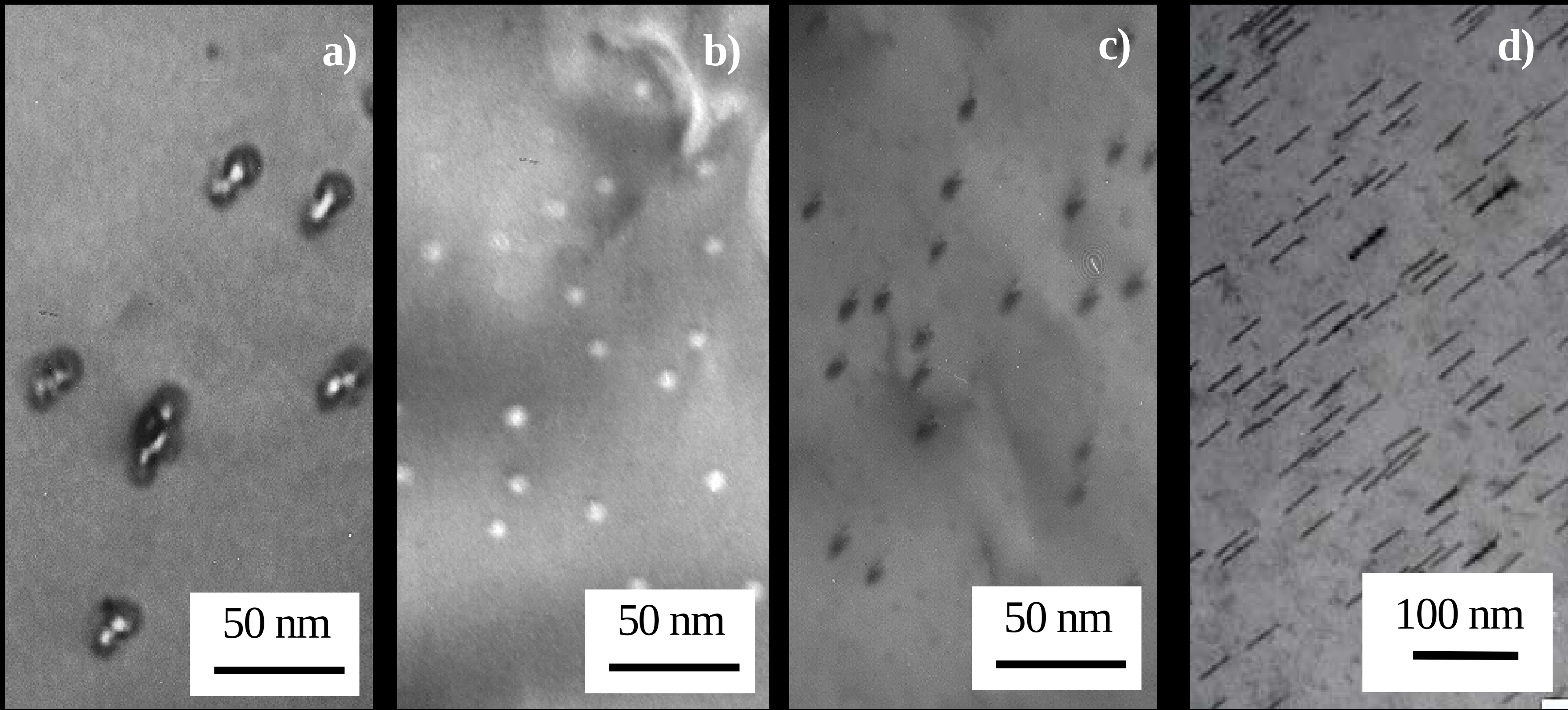


a) 30 MeV $C_{60}$ Buckminster fullerenes b) 2.38 GeV Bi-ions

c) 120 MeV Bi-ions d) 70 MeV I-ions (specimen tilted in the electron beam)

Wiss, T., Matzke, Hj., Heavy ion induced damage in MgAl2O4, an inert matrix candidate for the transmutation of minor actinides 1999 Radiation Measurements 31 (1), pp. 507-514

# Recrystallization of $MgAl_2O_4$

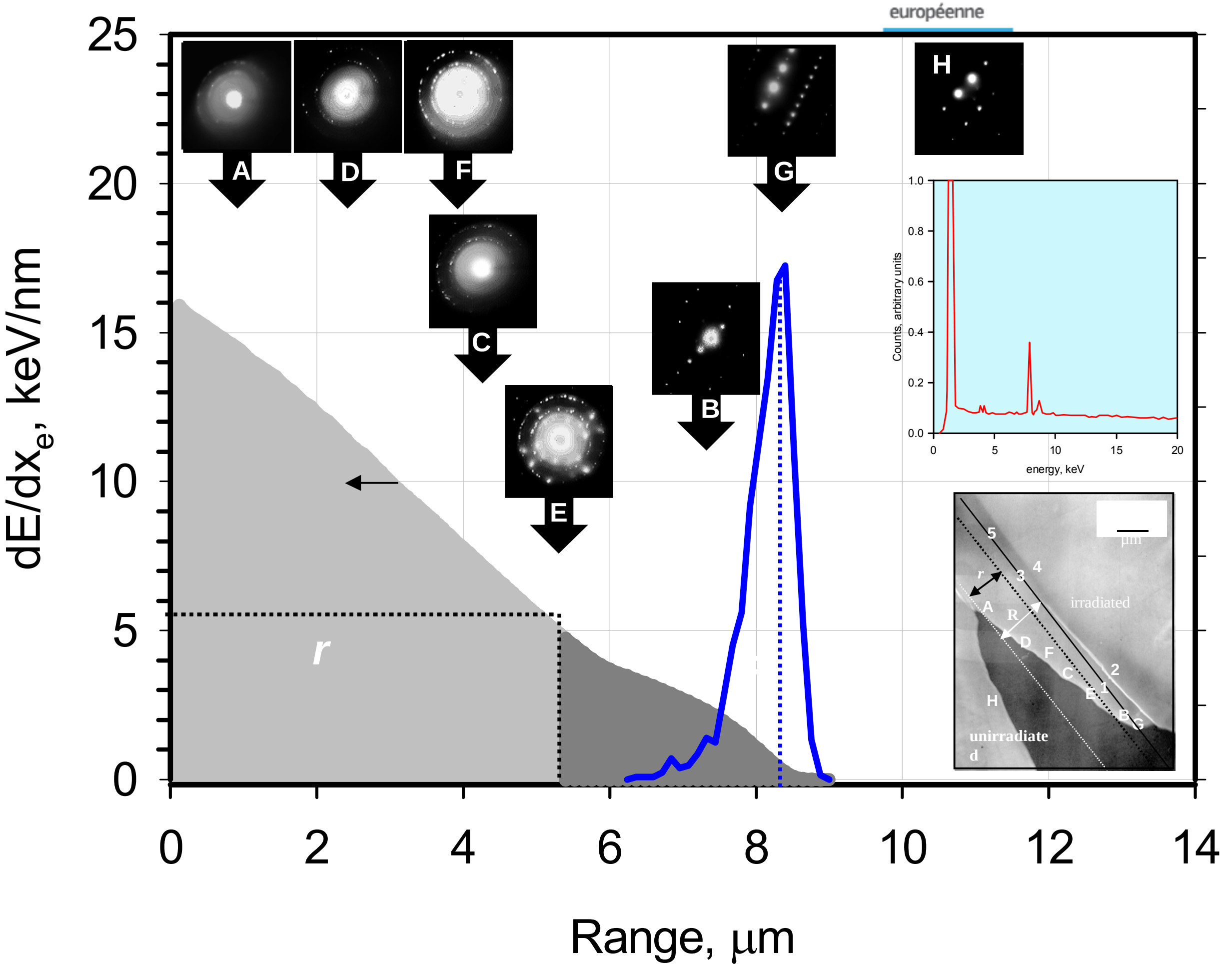


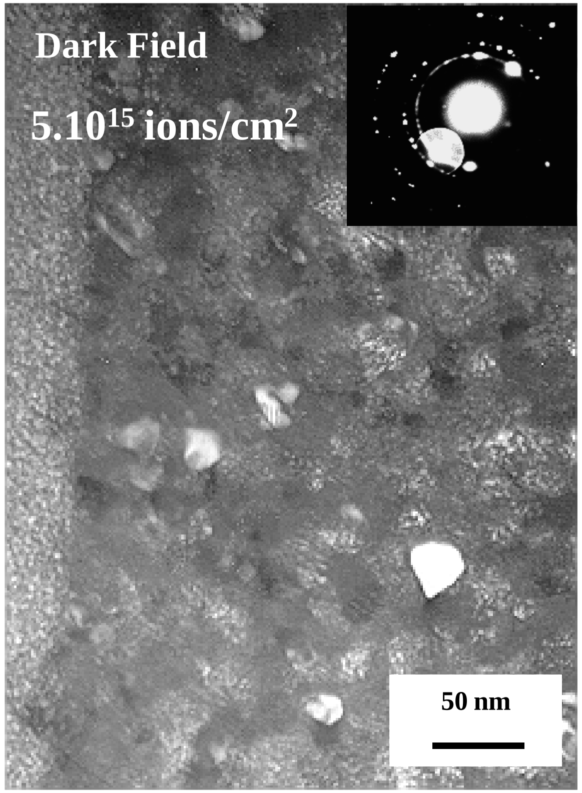


A cross-sectional TEM - dE/dx - study has allowed to determine the amorphization threshold (6 keV/nm) of spinel for fission products (iodine 72 MeV)

# TEM observation on track formation

Commission européenne

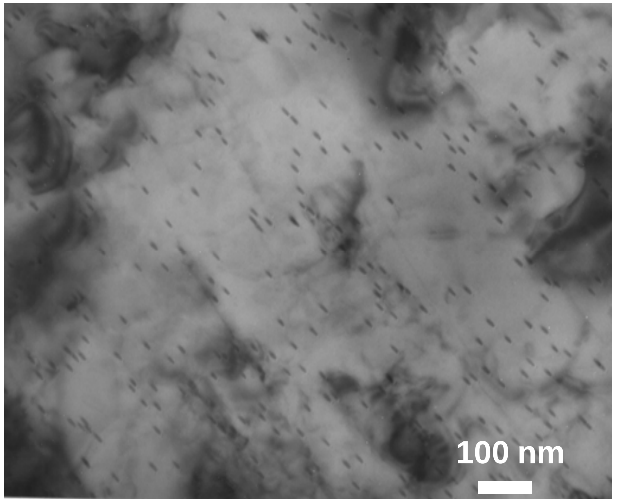


1.3 GeV $^{213}Bi$ in spinel

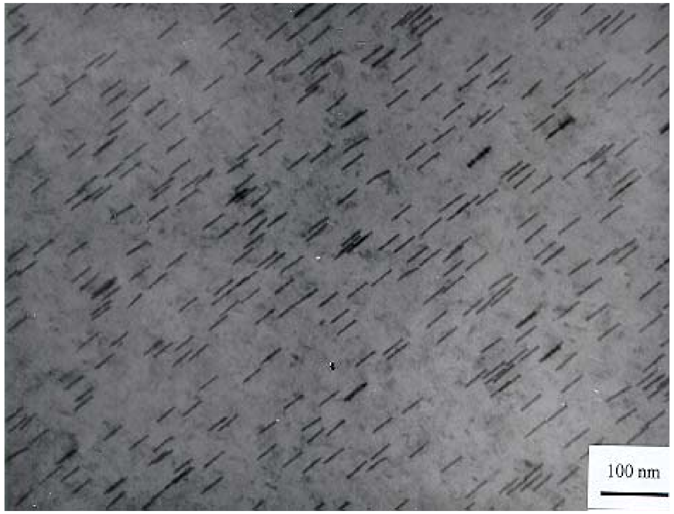


70 MeV $^{127}I$ in spinel

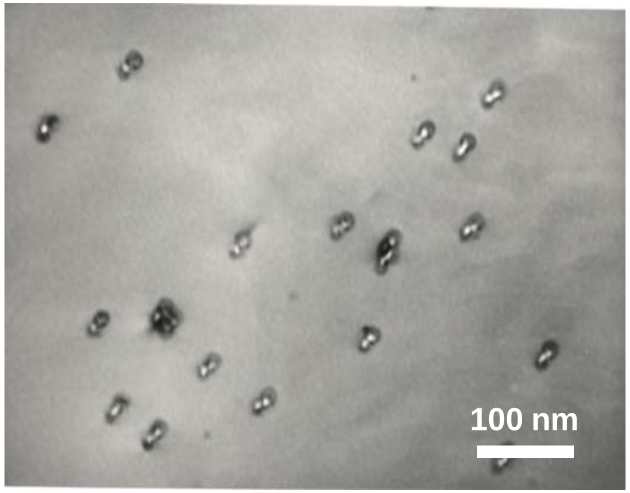


30 MeV $C_{60}$ in spinel

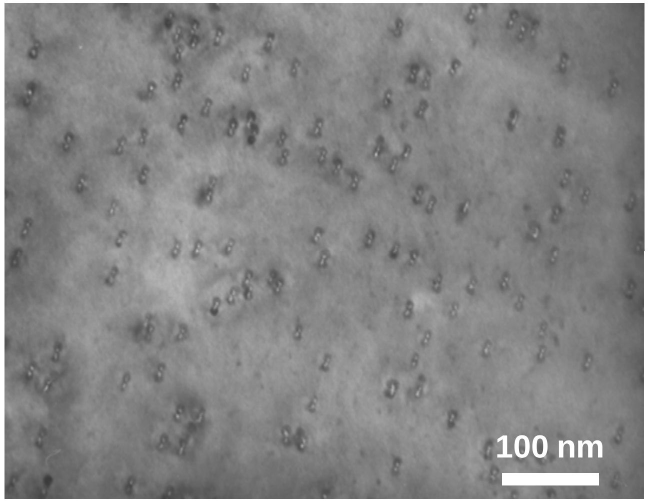


70 MeV $^{127}I$ in ceria

Joint Research Centre

# Damage by energetic ions in spinel

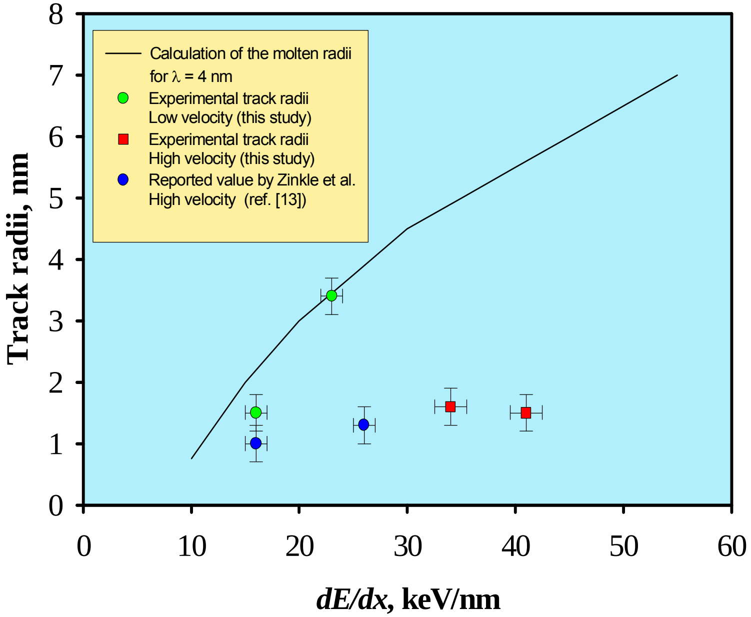


Calculation of the molten radii along swift heavy ion tracks using a thermal spike model

dE/dx threshold for track formation:
6.6 keV/nm (calculated)

Ion tracks:

-Low velocity (1 MeV/amu, FPs) largest track radii.
Well fitted for l = 4 nm supporting the assumption of a melt phase around the ion path.
- Medium velocity (5 MeV/amu) lower track radii.
- High velocity (>10 MeV/amu) smaller track radii observed in spinel.

The deposited **energy density** is the key parameter for track radii.

Irradiations with FPs, Amorphization, Swelling
After exposure to $e^-$: Recrystallization: formation of irradiation-induced nanostructures

# EFFTRA-T4

Commission européenne

$MgAl_2O_4$ selected according its properties ($\lambda$, $\sigma_n$, resistance to damage (n, $\alpha$), $T_m$, etc)

**Study of a once through scenario in an (epi) thermal flux (HFR)**

Infiltration of 11 wt% $^{241}Am$

Irradiation: 358 FPDs, T < 1050 K, fission power 30 – 270 $W.cm^{-3}$

Swelling 18 % due to gas production (He;$10^{-3}$ $mol/cm^3$ ; 4400appm)

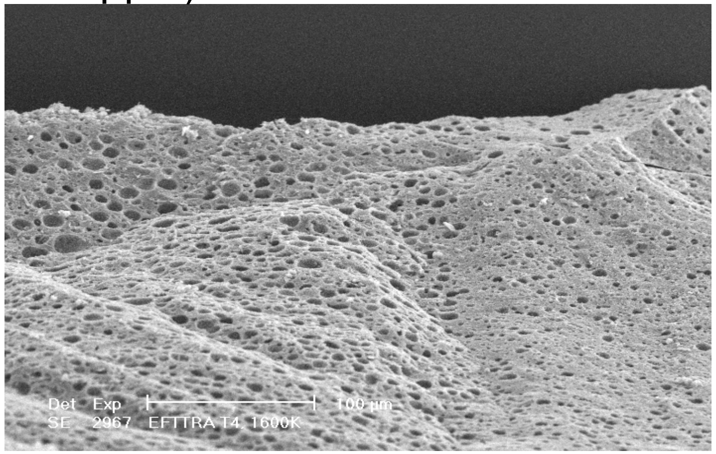


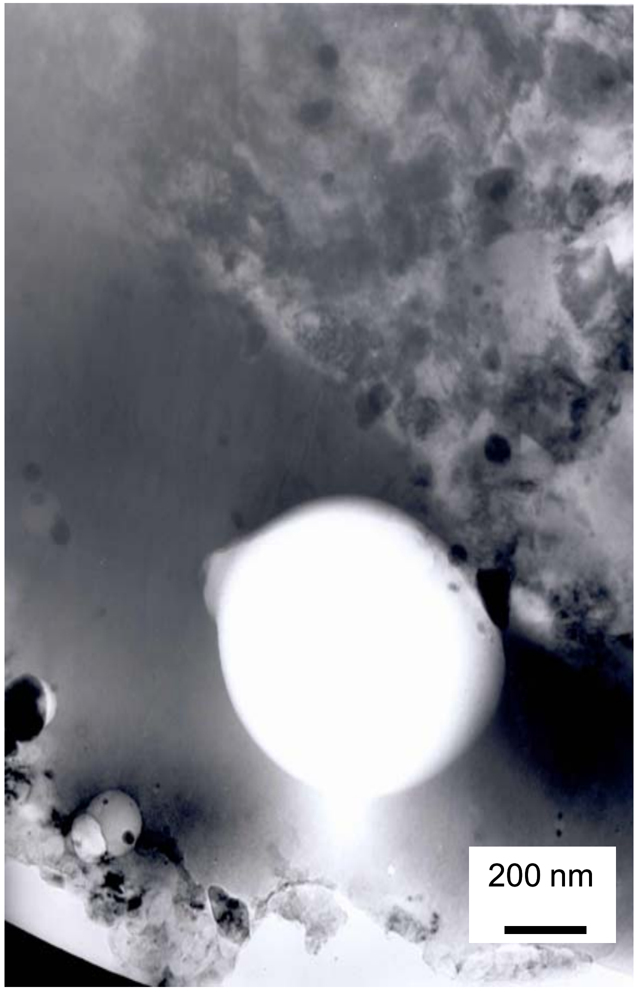


Wiss, T., Konings, R.J.M., Walker, C.T., Thiele, H., 2003, Journal of Nuclear Materials 320 (1-2), pp. 85-95

# Optimization of IMF with spinel

Commission européenne

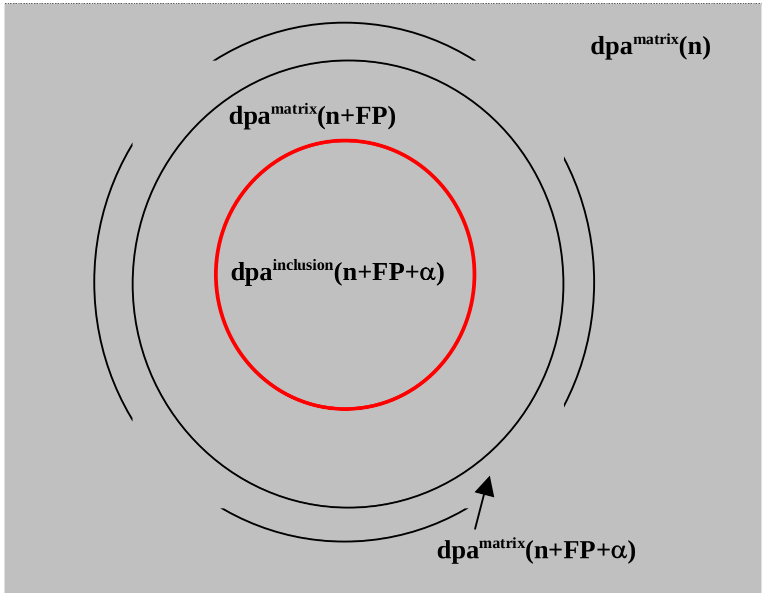


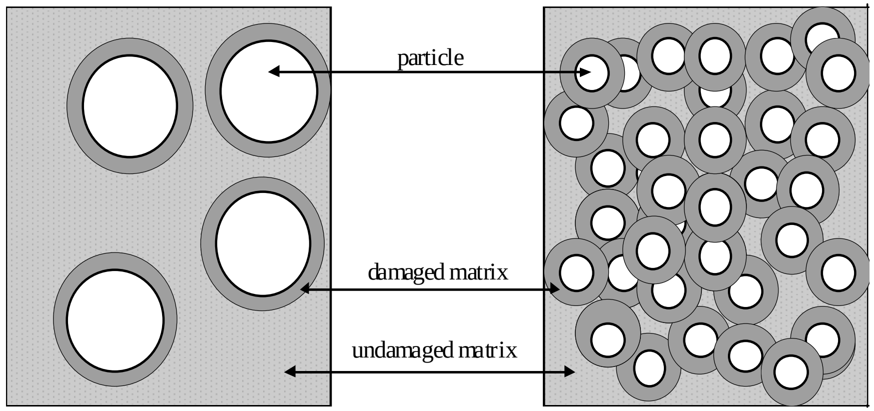


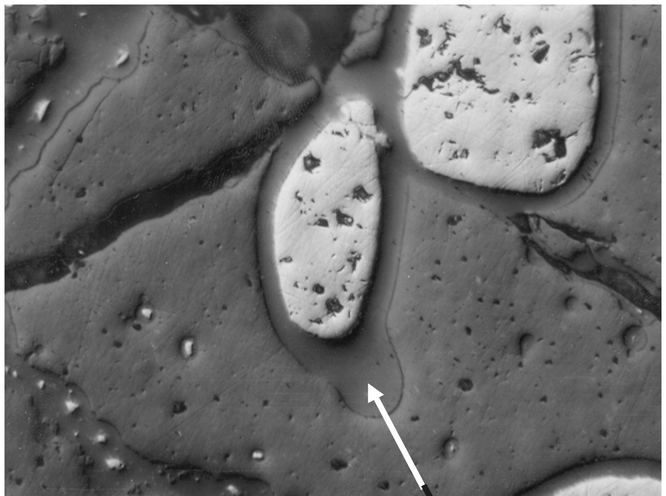

Fissile inclusion ($UO_2$)

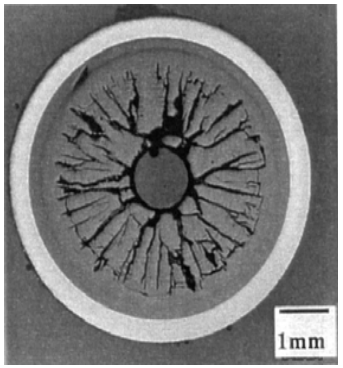


Micro -

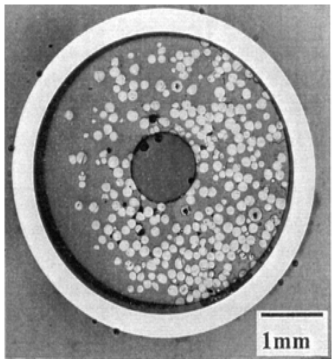


Macro -

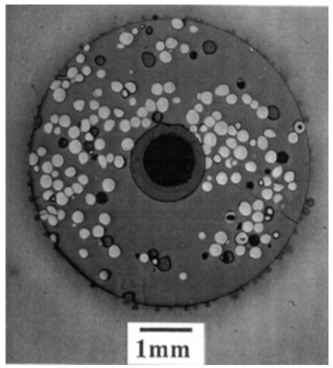


Jingle -

Joint Research Centre

# Conclusions on spinel as IMF

Commission européenne

- Information available for $MgAl_2O_4$-based fuel is extensive.
- The number of studies certainly exceeds those for most alternatives.
- Further conclusions on the usefulness of $MgAl_2O_4$ for this specific application must wait for the results of equally detailed studies on alternative materials.
- Chemical and poor radiation stability (FPs) makes it a poor IMF candidate.

# Waste Conditioning Matrices

# Zirconolites

Commission européenne

## Zirconolite $CaZrTi_2O_7$

Main constituent of **SYNROC©** developed at ANSTO: can accommodate Ln and tri- and tetravalent An in the Ca and Zr sites (monoclinic structure). Natural zirconolites have the ability to incorporate up to 24 wt% $UO_2$, 22 wt% $ThO_2$, and 32 wt% $REE_2O_3$ in the structure.

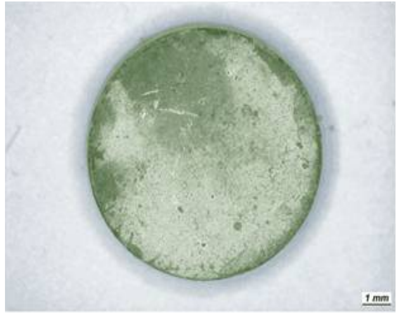

$^{239}$Pu-doped

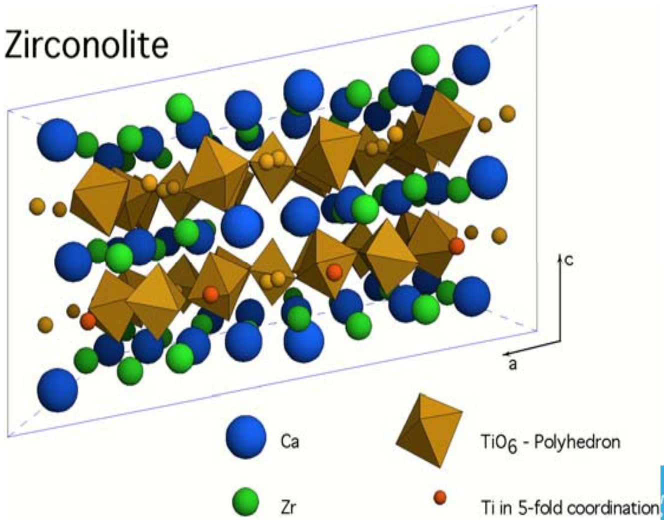


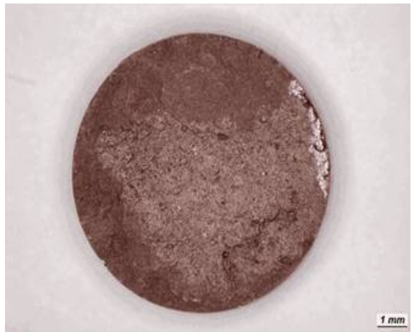

$^{238}$Pu-doped

# Helium release from doped zirconolites

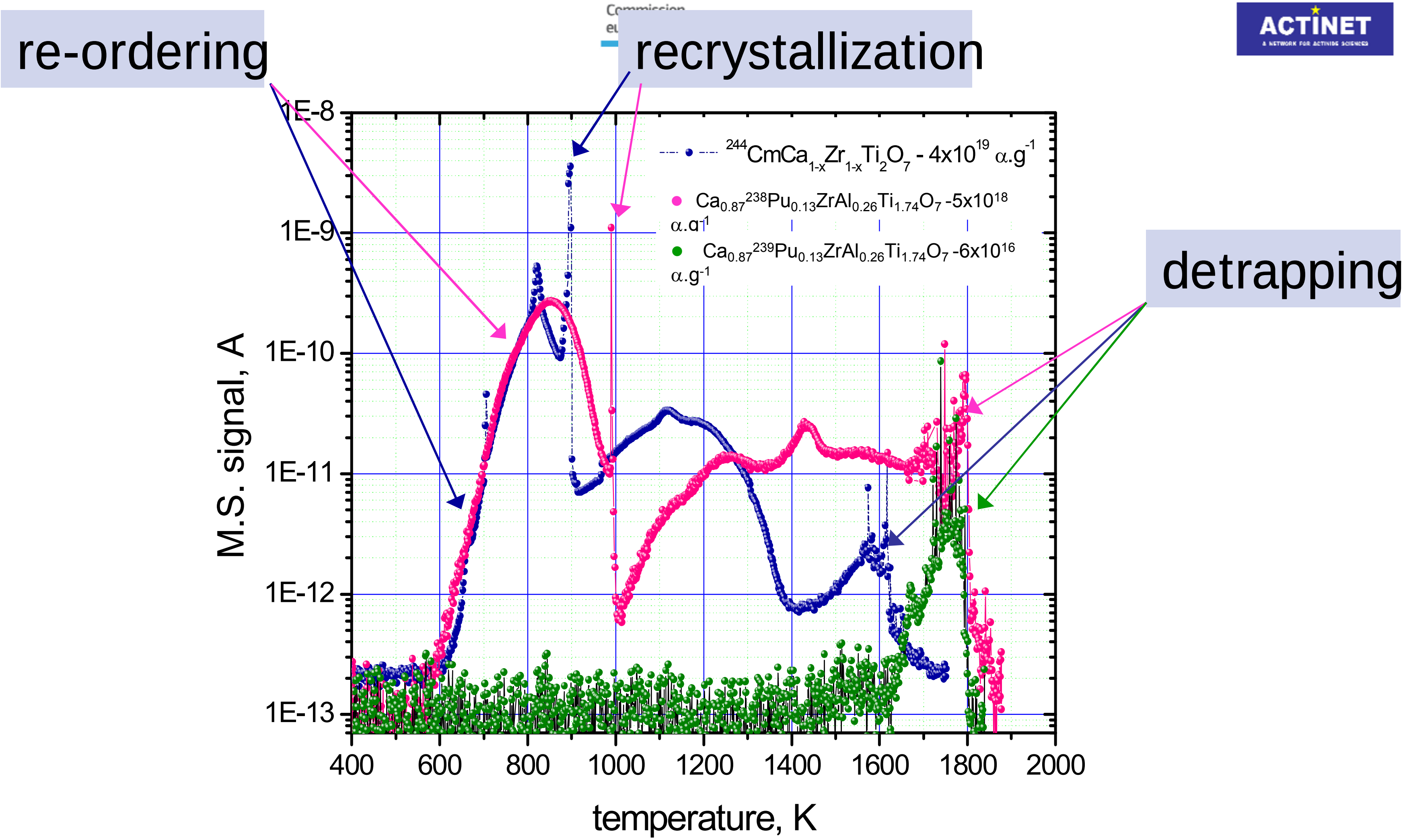


**rhombohedral → monoclinic → monoclinic + hexagonal (3T)**

Wiss, T.A.G., Hiernaut, J.-P., Damen, P.M.G., Lutique, S., Fromknecht, R., Weber, W.J., Helium behaviour in waste conditioning matrices during thermal annealing, 2006, Journal of Nuclear Materials 352 (1-3), pp. 202-208

# Annealing of $^{244}CmCa_{1-x}Zr_{1-x}Ti_2O_7$

Commission européenne

Bruker D8 X-ray diffractometer

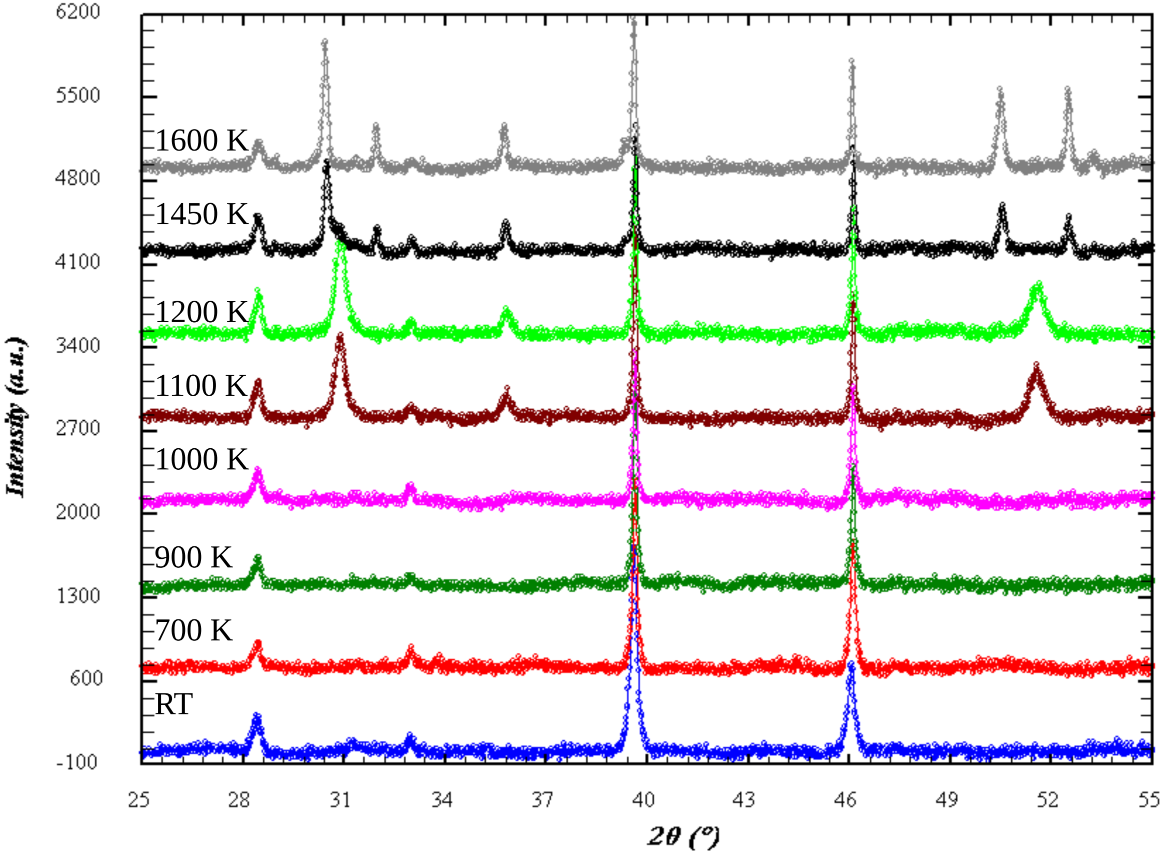


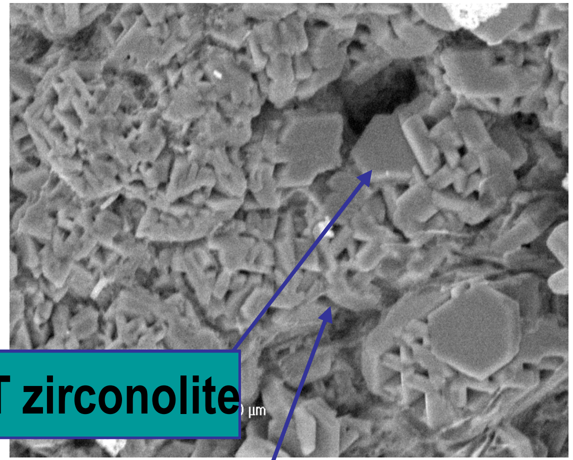

3T zirconolite

Monoclinic

Amorphous

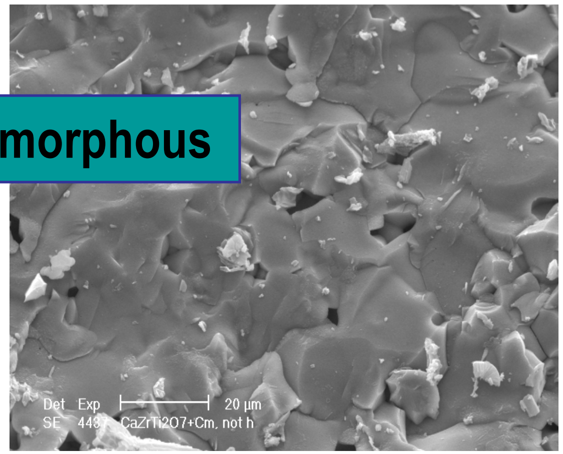


ACTINET

Joint Research Centre

# Conclusions

Commission européenne

The Fractional Release data show that the onset of significant He-release is closely associated with the onset of recrystallization and densification.

The integrity of the studied materials was preserved during storage.

The following sequence could be drawn from the different investigations on the phase transition of 2M-zirconolite during damage build-up and recovery: monoclinic – pyrochlore – fluorite – amorphous- rhombohedral – monoclinic (+ pseudo hexagonal).

this study on helium behaviour shows the ability for this type of compound to accommodate for large quantities of helium.

# Aknowledgements

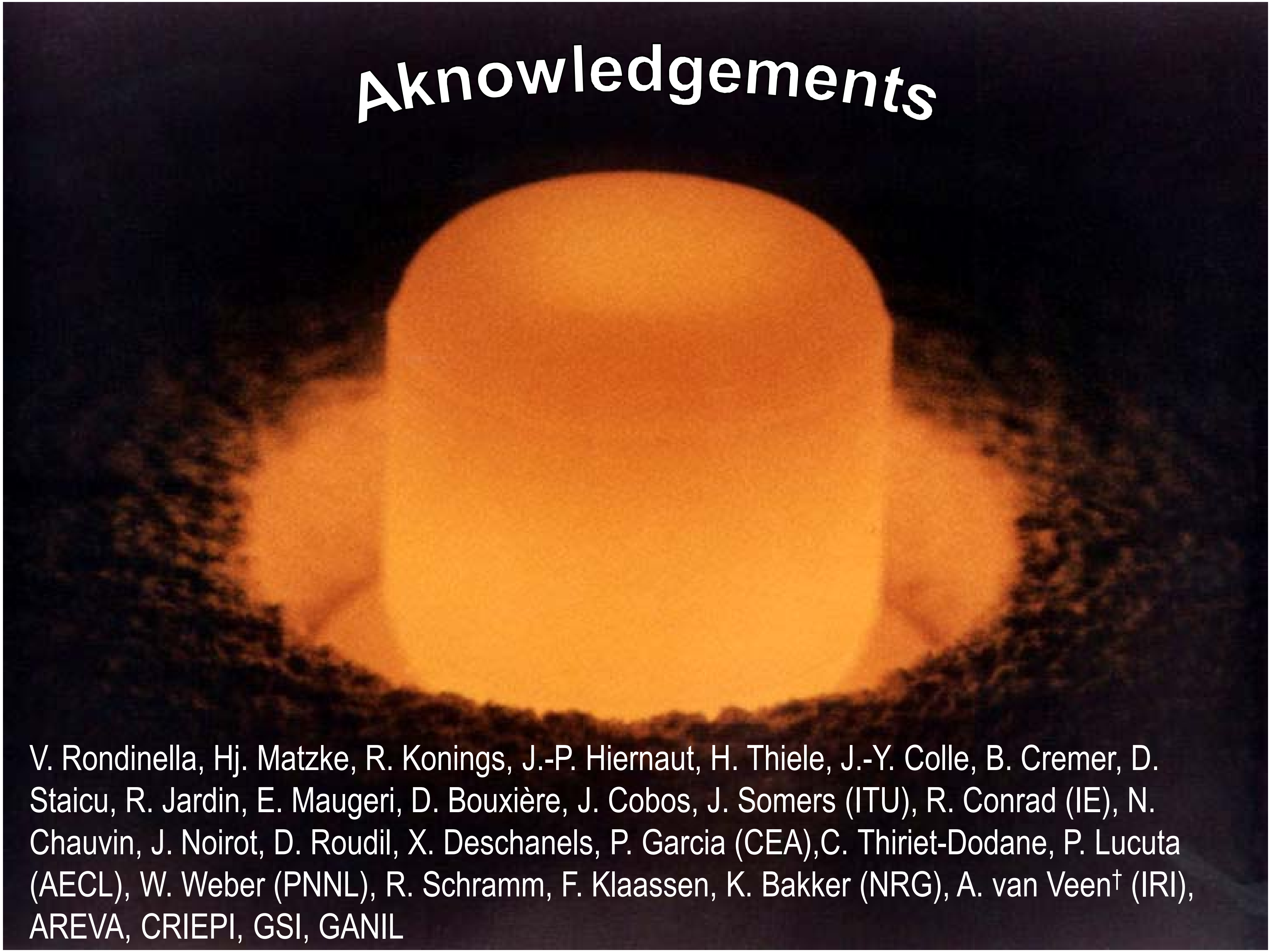

V. Rondinella, Hj. Matzke, R. Konings, J.-P. Hiernaut, H. Thiele, J.-Y. Colle, B. Cremer, D. Staicu, R. Jardin, E. Maugeri, D. Bouxière, J. Cobos, J. Somers (ITU), R. Conrad (IE), N. Chauvin, J. Noirot, D. Roudil, X. Deschanels, P. Garcia (CEA),C. Thiriet-Dodane, P. Lucuta (AECL), W. Weber (PNNL), R. Schramm, F. Klaassen, K. Bakker (NRG), A. van Veen† (IRI), AREVA, CRIEPI, GSI, GANIL

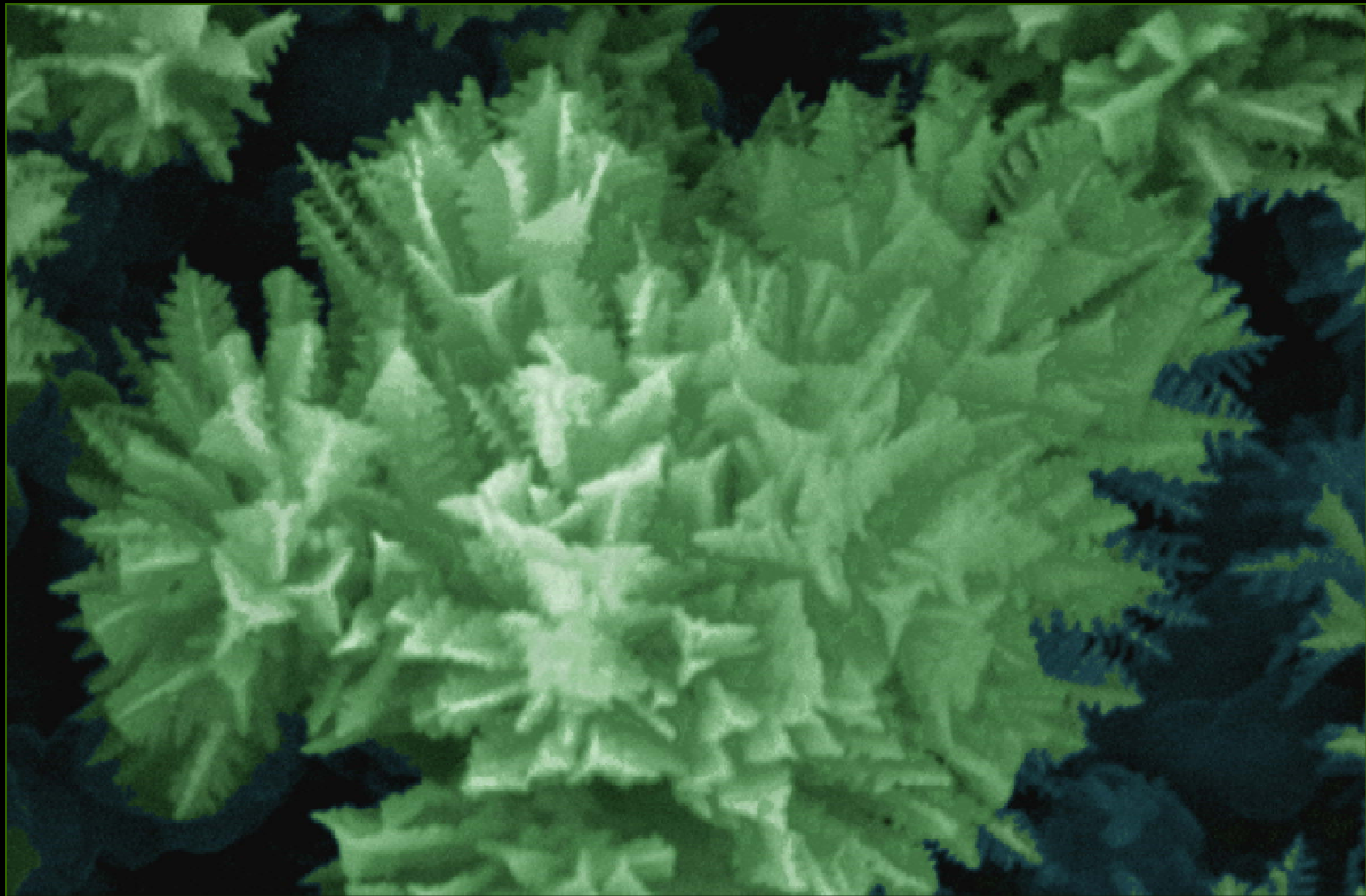

Thank you for your attention !

# Particle / ion-matter interactions

Commission européenne

Slowing down of a particle/ion in a target

- history of the particle
  energy loss of a particle, range, interactions

- history of the target atoms
  displacements, recombinations, ionization, excitation, radiation damage build-up

Areas of interest

Nuclear industry, nuclear medicine, space applications, semi-conductor, geology...

# Rutherford diffusion

Commission européenne

## Classical description of a two-particles interaction as a function of impact parameter b, diffusion angle θ, and solid angle Ω.

### Classical approach

Non relativistic particle, Mass center ≡ Lab. Ref., Coulombic force

$$\vec{F} = \frac{1}{4\pi\varepsilon_0}\frac{Z_1 Z_2 e^2}{r^2}\vec{\mu}_r$$

$$\frac{1}{2}M_1 v_1^2 = \frac{1}{4\pi\varepsilon_0}\frac{Z_1 Z_2 e^2}{D}$$

$$p = \int F dt = \int_{-\infty}^{+\infty}\frac{F}{v_1}dx = \frac{Z_1 Z_2 e^2}{4\pi\varepsilon_0}\int_{-\infty}^{+\infty}\frac{dx}{v_1\left(x^2+b^2\right)}$$

$$\Delta G = Q = \frac{p^2}{2M_2} = \frac{2\left(Z_1 Z_2 e^2\right)^2}{\left(4\pi\varepsilon_0\right)^2 M_2 v_1^2 b^2}$$

Cross-section for diffusion

$$\sigma\left(>\theta_0\right) = \pi b^2$$

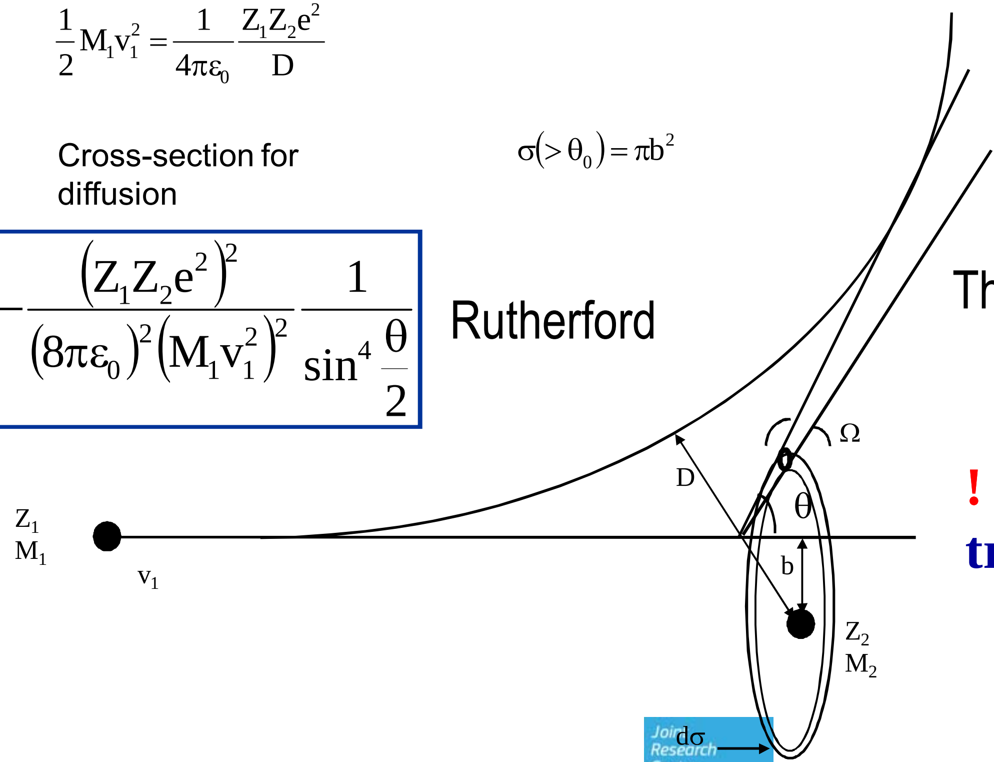


$$\frac{d\sigma}{d\Omega} = -\frac{\left(Z_1 Z_2 e^2\right)^2}{\left(8\pi\varepsilon_0\right)^2\left(M_1 v_1^2\right)^2}\frac{1}{\sin^4\frac{\theta}{2}}$$

Rutherford

Thomson

$$\frac{d\sigma}{dQ} = -\frac{\left(Z_1 Z_2 e^2\right)^2}{8\pi\varepsilon_0^2 M_2 v_1^2 Q^2}$$

**! dσ ≡ $1/Q^2$, low energy tranfer**

**$1/M_2$, mainly on $e^-$**

**$1/v_1$, end of range**

Joint Research Centre

# Rutherford diffusion

## ….In fact..

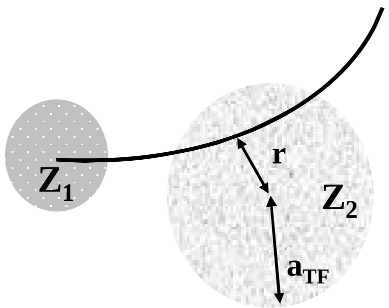


**Screening by e⁻ : Thomas-Fermi potential**

$$V(r) = \Phi\left(\frac{r}{a_L}\right)\frac{Z_1 Z_2 e^2}{r}$$

with the screening function $\Phi$
and screening length (Lindhard)

$$a_L = \frac{0.8853}{\left(Z_1^{2/3} Z_2^{2/3}\right)^{1/2}} a_0$$

## Interatomic potential

Other description of the screening function
by Lenz, Jensen, Sommerfeld, Moliere

Inter-penetration of the electron clouds
Hartree-Fock-Slater calculations.
However, good approximation by TF

## Charge distribution in single atom

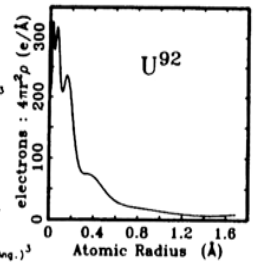


$U^{92}$

Atomic Number ......... 92
Atomic Weight ......... 238 amu
Mass Density .......... 19 g/cm³
Atomic Density ........ 0.0482 Atoms/Ang.³
Lattice Type .......... ORC
Lattice Constant ...... 2.85 Ang.
2nd Lattice Constant... 1.88 Ang.
Muffin-Tin Radius ..... 1.45 Ang.
Fermi Velocity-Theory (Cont).. 1.03 Vo
Fermi Velocity-Theory (Disc).. 1.01 Vo
Fermi Velocity-Experiment..... None Avail.
Interstititial Volume... 7.99 (Ang.)³
Interstititial Charge... 1.89 electrons
Interstititial Density (Disc) .. 0.238 e/(Ang.)³

| Rad. (A) | Chg.(e/A³) | Rad. (A) | Chg.(e/A³) | Rad. (A) | Chg.(e/A³) | Rad. (A) | Chg.(e/A³) |
|---|---|---|---|---|---|---|---|
| 0.00104 | 2.65E6 | 0.0477 | 9.82E3 | 0.255 | 122 | 1.32 | 0.342 |
| 0.00207 | 1.85E6 | 0.0519 | 8.57E3 | 0.272 | 93.3 | 1.45 | 0.246 |
| 0.00311 | 1.30E6 | 0.056 | 7.62E3 | 0.288 | 75.8 | 1.46 | 0.246 |
| 0.00415 | 9.12E5 | 0.0601 | 6.82E3 | 0.305 | 64.5 | 1.47 | 0.246 |
| 0.00519 | 6.47E5 | 0.0643 | 6.07E3 | 0.355 | 46.8 | 1.49 | 0.246 |
| 0.00622 | 4.64E5 | 0.0684 | 5.37E3 | 0.388 | 38.1 | 1.5 | 0.246 |
| 0.00726 | 3.40E5 | 0.0726 | 4.70E3 | 0.421 | 30 | 1.51 | 0.246 |
| 0.0083 | 2.54E5 | 0.0809 | 3.52E3 | 0.454 | 23 | 1.52 | 0.246 |
| 0.00933 | 1.98E5 | 0.0892 | 2.60E3 | 0.487 | 17.3 | 1.54 | 0.246 |
| 0.0104 | 1.56E5 | 0.0975 | 1.95E3 | 0.521 | 12.9 | 1.55 | 0.246 |
| 0.0124 | 1.10E5 | 0.106 | 1.53E3 | 0.554 | 9.68 | 1.56 | 0.246 |
| 0.0145 | 8.62E4 | 0.114 | 1.27E3 | 0.587 | 7.41 | 1.57 | 0.246 |
| 0.0166 | 7.27E4 | 0.122 | 1.11E3 | 0.62 | 5.83 | 1.59 | 0.246 |
| 0.0187 | 6.31E4 | 0.131 | 1.01E3 | 0.653 | 4.72 | 1.6 | 0.246 |
| 0.0207 | 5.51E4 | 0.139 | 9.25E2 | 0.72 | 3.33 | 1.61 | 0.246 |
| 0.0228 | 4.80E4 | 0.147 | 8.50E2 | 0.786 | 2.52 | 1.62 | 0.246 |
| 0.0249 | 4.15E4 | 0.156 | 7.75E2 | 0.852 | 1.95 | 1.63 | 0.246 |
| 0.027 | 3.56E4 | 0.172 | 6.17E2 | 0.919 | 1.51 | 1.65 | 0.246 |
| 0.029 | 3.04E4 | 0.189 | 4.65E2 | 0.985 | 1.16 | 1.66 | 0.246 |

Commission européenne
Joint Research Centre

# The stopping power

Commission européenne

## Electronic stopping power

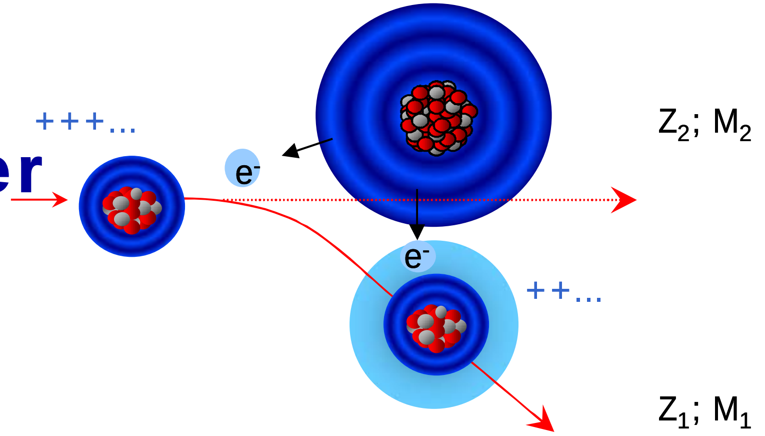


Electronic collisions constitutes inelastic interactions where electrons can be exchanged between incident ions and target atoms. The corrected Bethe and Bloch
formula is adequate for particle velocity larger than the velocity of the minimum-bound
electrons.

$$-\left.\frac{dE}{dx}\right)_e = nZ_2 \frac{4\pi}{m_e v_2^2}\left(\frac{Z_1^* e^2}{4\pi\varepsilon_0}\right)^2\left[\ln\left(\frac{2mv^2}{I}\right) - \beta^2 - \ln\left(1-\beta^2\right) - \frac{C}{Z^2}\right]$$

For lower velocities the electron clouds can re-organize them. Lindhard and Scharff proposed an expression for the electronic stopping power based on the TF atom

$$V_1 << Z_1^{2/3} V_0$$

$$-\left.\frac{dE}{dx}\right)_e = N_A Z_1^{1/6} \times 8\pi r_B e^2 \times \frac{Z_1 Z_2}{\left(Z_1^{2/3} Z_2^{2/3}\right)^{3/2}} \times \frac{V_1}{V_2}$$

Joint Research Centre

# The stopping power

Electronic energy losses produce thermal spike + shock waves resulting in surface track formation.

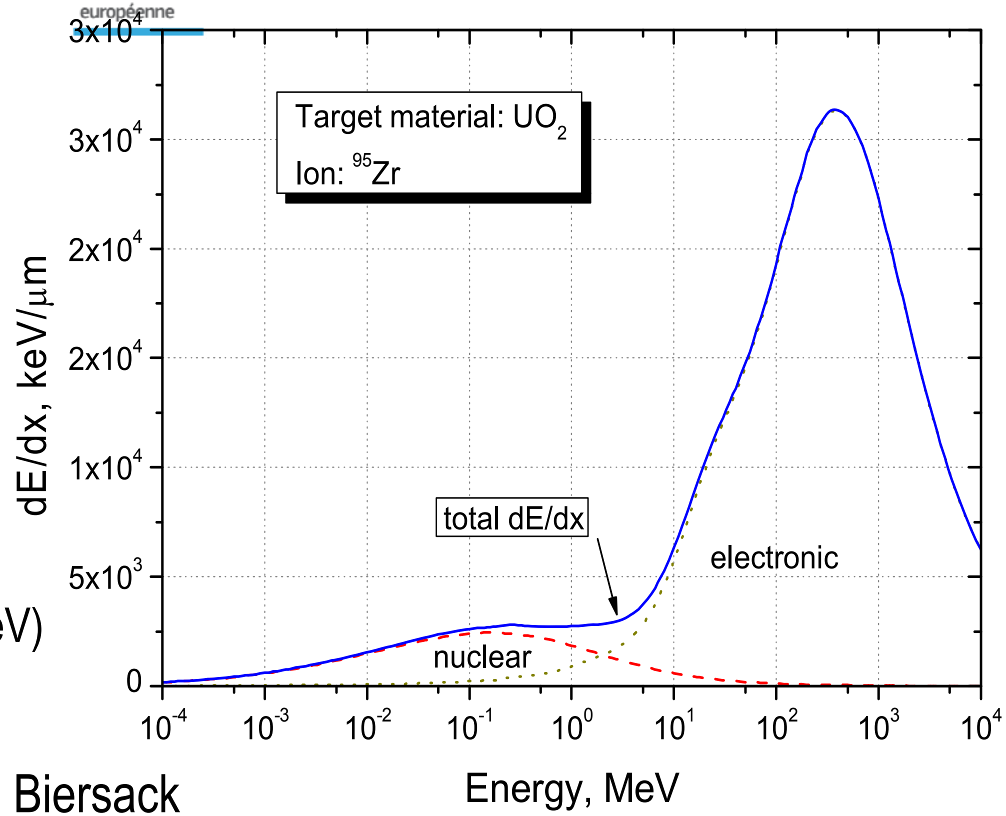


## Nuclear stopping power

(Below 0.1 MeV)

$$-\left(\frac{dE}{dx}\right)_n = T.d\sigma_s(E_1,T) = 4\pi N a_{TF}\left(\frac{M_1}{M_1+M_2}\right)Z_1Z_2e^2\frac{\log(\varepsilon)}{2\varepsilon\left(1-\varepsilon^{-1.49}\right)}$$

Biersack

## Electronic stopping power

$$-\left(\frac{dE}{dx}\right)_e = nZ_2\frac{4\pi}{m_e v_2^2}\left(\frac{Z_1^* e^2}{4\pi\varepsilon_0}\right)^2\left[\ln\left(\frac{2mv^2}{I}\right)-\beta^2-\ln\left(1-\beta^2\right)-\frac{C}{Z^2}\right]$$

Bethe & Bloch


SRIM: Ziegler, J. F., Biersack, J.P., Littmark, U., The Stopping and Range of Ions in Solids, Pergamon Press, Oxford, 1985

# Effective charge and stopping power

Commission européenne

Effective charge $Z_1^*$ - dependence on the velocity

$$Z_1^* = \frac{Z_1^{1/3} V_1}{V_0} \quad \text{if} \quad V_1 < V_0 Z_1^{2/3} \qquad -\frac{dE}{dx}\bigg) \propto \sqrt{E}$$

$$Z_1^* = Z_1 \quad \text{if} \quad V_1 >> V_0 Z_1^{2/3} \qquad -\frac{dE}{dx}\bigg) \propto \frac{\log E}{E}$$

Maximum stopping power - Bragg peak

$$V_1 \approx V_0 Z_1^{2/3} \qquad -\frac{dE}{dx}\bigg) \propto \log E$$

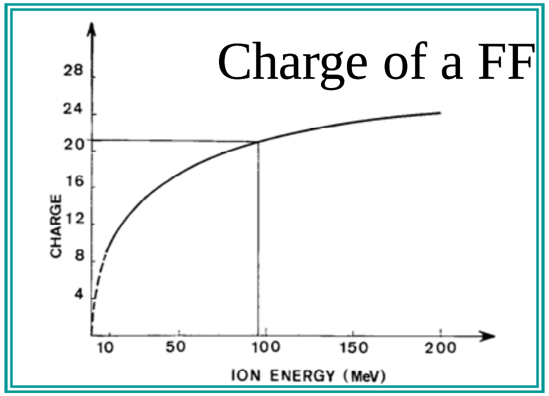


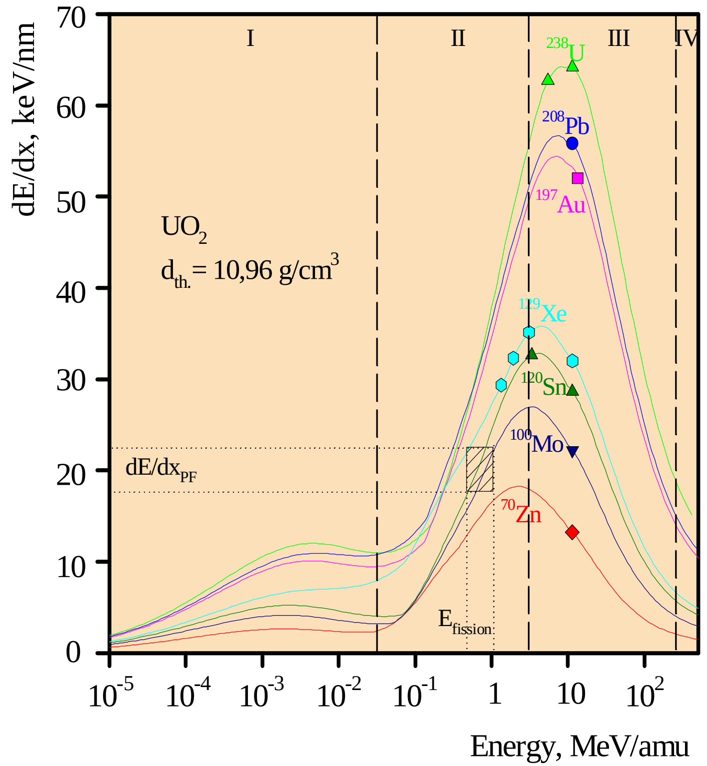


| Domain | Velocity |
|---|---|
| I | $v << Z_1 v_0$ |
| II | $v \cong Z_1 v_0$ |
| III | $Z_1 v_0 < v < c$ |
| IV | $v \cong c$ |

$v_O$ = Bohr velocity (electron in hydrogen) = $2.19 \cdot 10^8$ cm/s

Joint Research Centre

# Nucl., Elec. stopping power and range for 2FPs

The range can be deduced by integrating the invert of dE/dx

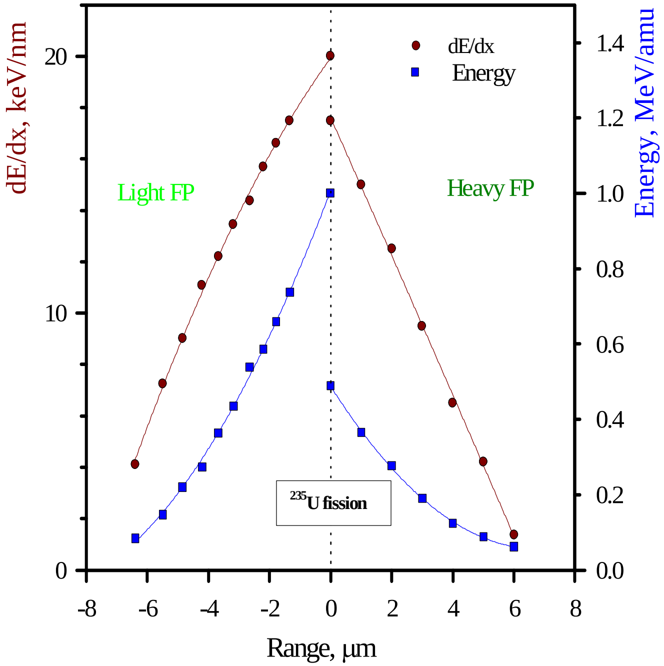


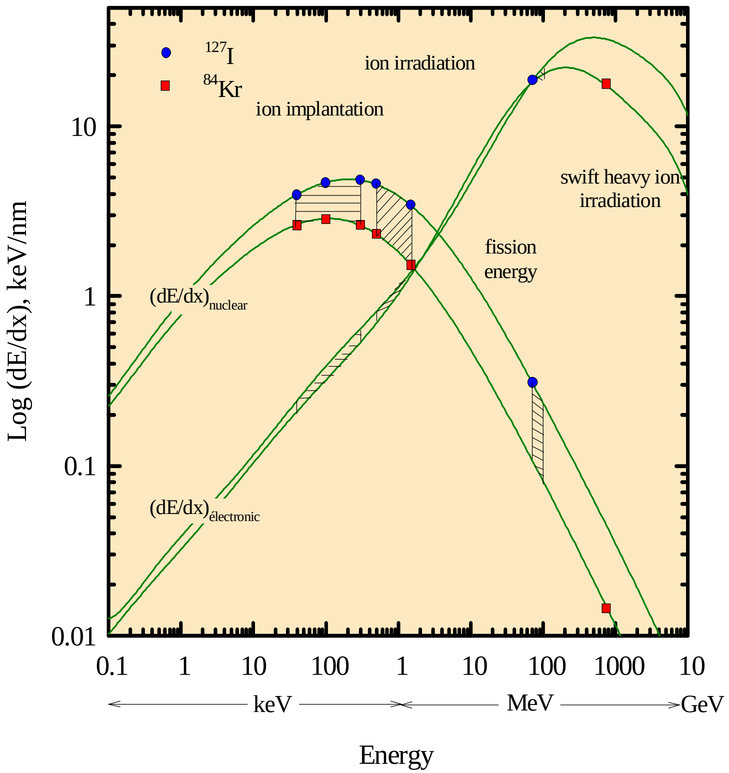


Maximum $dE/dx)_n$ for 0.1 MeV
Maximum $dE/dx)_e$ for ~ 400 MeV

# Energy loss in $UO_2$



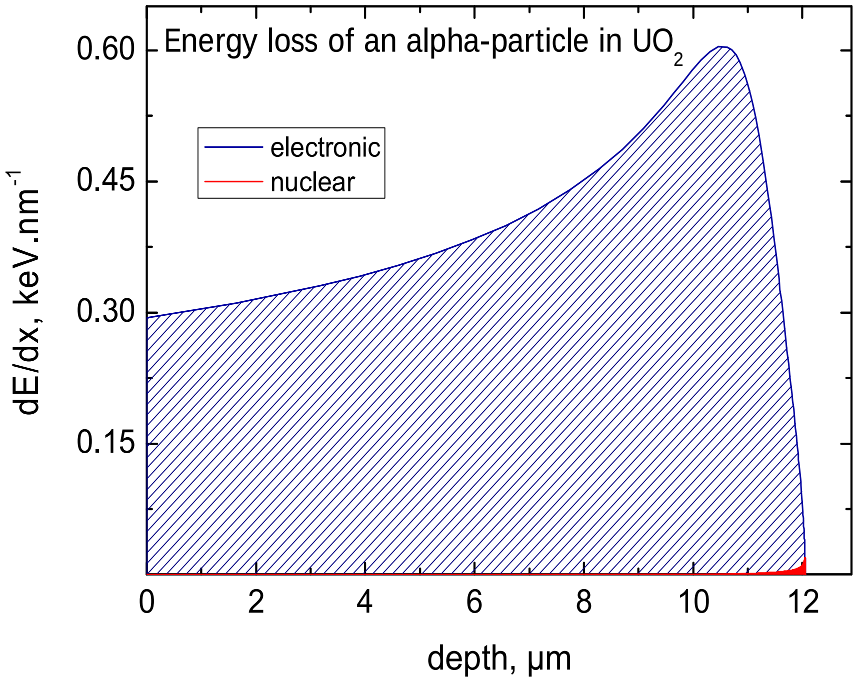


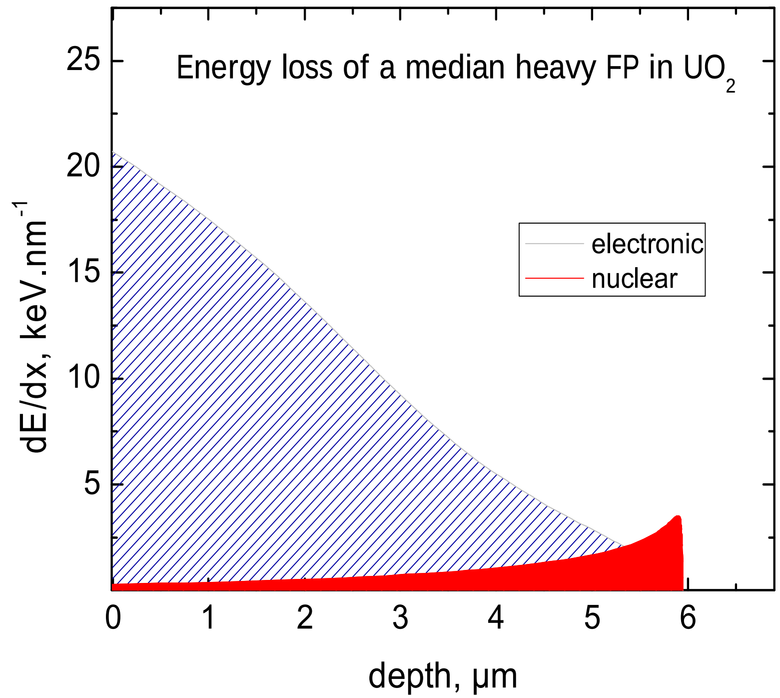


**SRIM: Ziegler, J. F., Biersack, J.P., Littmark, U., The Stopping and Range of Ions in Solids, Pergamon Press, Oxford, 1985**

# Displacement energy - cascades

Commission européenne

Communication of kinetic energy to a lattice atom sufficient to break bonds
- lattice elastic forces cannot bring it back

☞ energy to transfer, $E_d$, threshold displacement energy.
☞ formation of a Frenkel pair

Dependence on lattice vibrations (Temperature), crystallographic directions.

If sufficient energy is transferred to the primary knock-on atom (pka) further collisions/displacements can occur.
☞ Displacement cascade

Number of displaced atom, n(T) per pka (Kinchin and Pease, 1955)

| | | |
|---|---|---|
| $n(T) = 0$ | if | $T < E_d$ |
| $n(T) = 1$ | if | $E_d < T < 2\,E_d$ |
| $n(T) = T/2\,E_d$ | if | $T \geq 2\,E_d$ |

Better approximation: $n(T) = 0.8\,(T - E_{ioniz})/2\,E_d$ for $T \geq 2\,E_d$

Joint Research Centre

# Defects creation in crystalline solids

Commission européenne

Linear defects:
- dislocations (screw, edge, mixed)

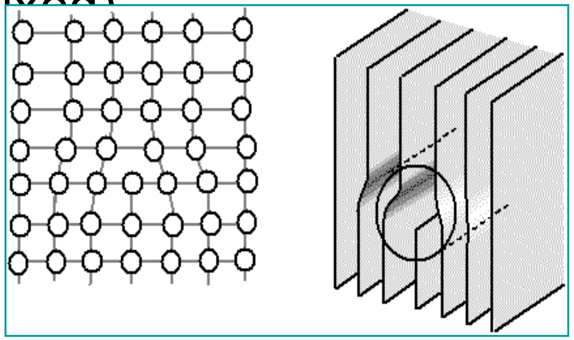

## Point defects

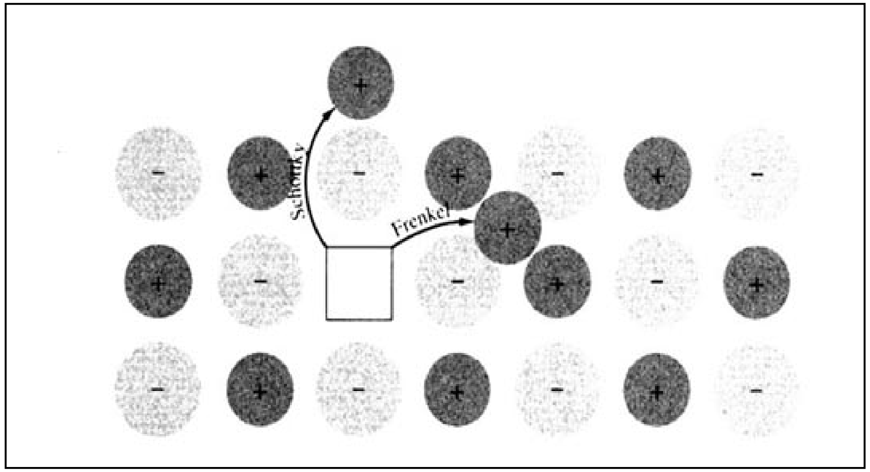


Bi-dimensional defects:
- stacking faults
- grain boundaries

Tri-dimensional defects:
- bubbles
- precipitates
- clusters

Vacancy $E^f_v \sim 1$ eV

Interstitial $E^f_i \sim 3\text{-}5$ eV

Frenkel pair: 4-6 eV

Substitutional

Defect concentration is T dependent

Joint Research Centre

# Stability of defects



Low temperature:

athermal recombination by newly produced defects
(overlap of displacement cascades)

Higher temperature:

migration of interstitials

- correlated recombination (interstitial with “its” vacancy)
- non-correlated recombination
- trapping on impurity
- trapping on sinks (dislocations, clustering)

The number of remaining defects is lower than the total number of displaced atoms.

e.g. in operating fuel values as high as 1500 **dpa** are reached during the fuel lifetime and the material remains crystalline !!

# Collision cascades in $UO_2$

Commission européenne

Alpha-particle 5.5 MeV

U-recoil 100 keV

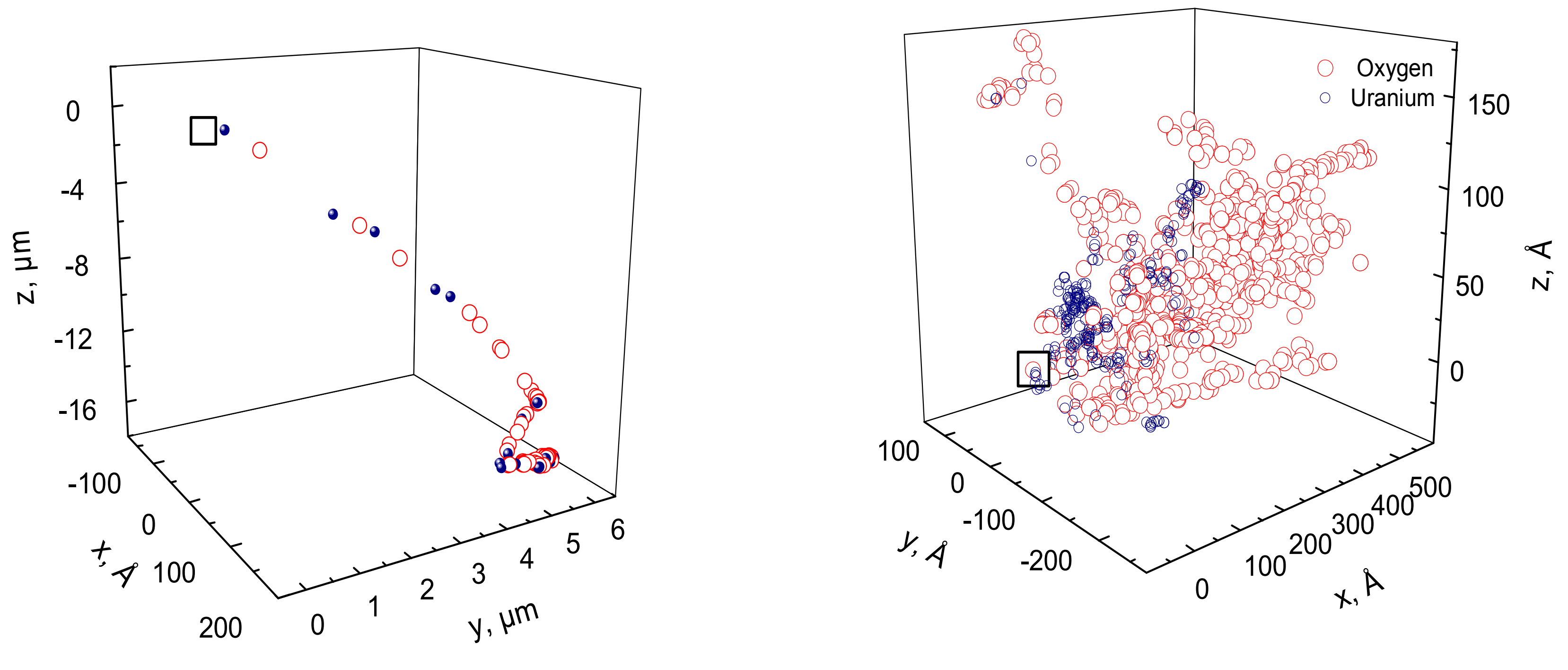


~ 150 displacements

~ 1500 displacements

SRIM: Ziegler, J. F., Biersack, J.P., Littmark, U., The Stopping and Range of Ions in Solids, Pergamon Press, Oxford, 1985

Joint Research Centre

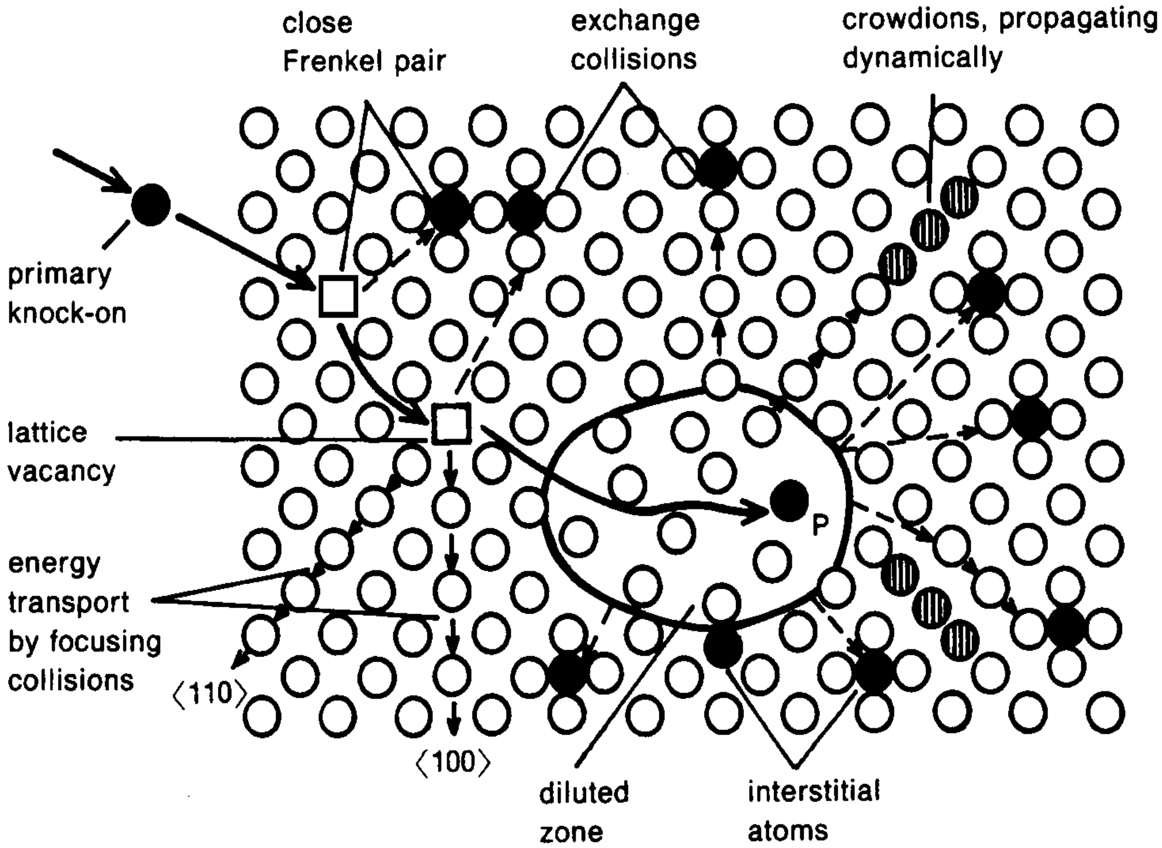
close
Frenkel pair
exchange
collisions
crowdions, propagating
dynamically
primary
knock-on
lattice
vacancy
energy
transport
by focusing
collisions
⟨110⟩
⟨100⟩
P
diluted
zone
interstitial
atoms

# The High Burnup Structure (HBS)

Commission européenne

- HBS (or RIM) structure is formed at high local burnup and low $T_{irr}$. It is characterized by grain subdivision, increased porosity, and evolves to an "ultimate" microstructure at very high burnup.
- No universal consensus on mechanisms and properties of HBS.
- However, it seems that HBS is not a negative feature of high burnup fuel:

    - *fg* is not released when HBS is formed

    - depletion of fission gases in the matrix, but almost complete retention in the fuel (rim porosity).

    - but release temperature decreases with decreasing $T_{irr.}$ and increasing burnup

Joint Research Centre

HBS

Optical | SEM | TEM

Std.

HBSI

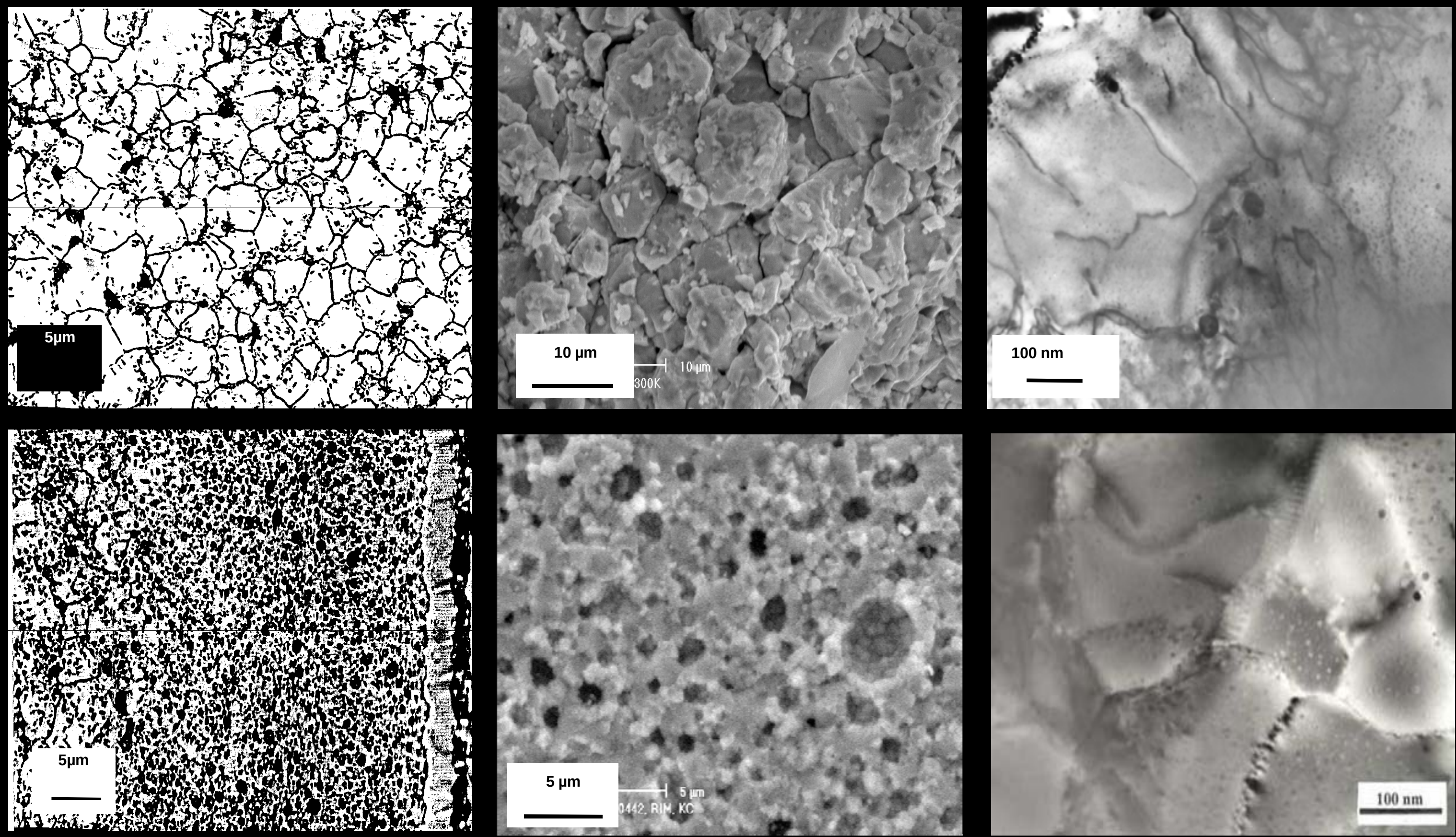

# High Burnup Structure

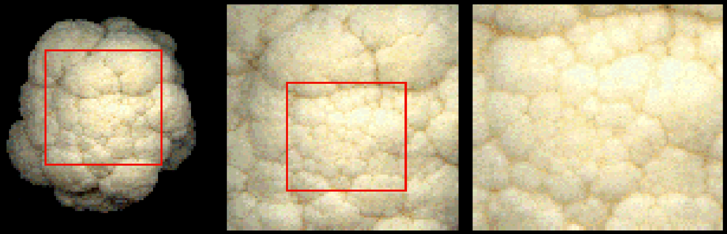

**Fractal dimension**

Log p / log q

p: nb of fractals

q: magnification

**HBS d= 2.2**

(Cauliflower d = 2.33)

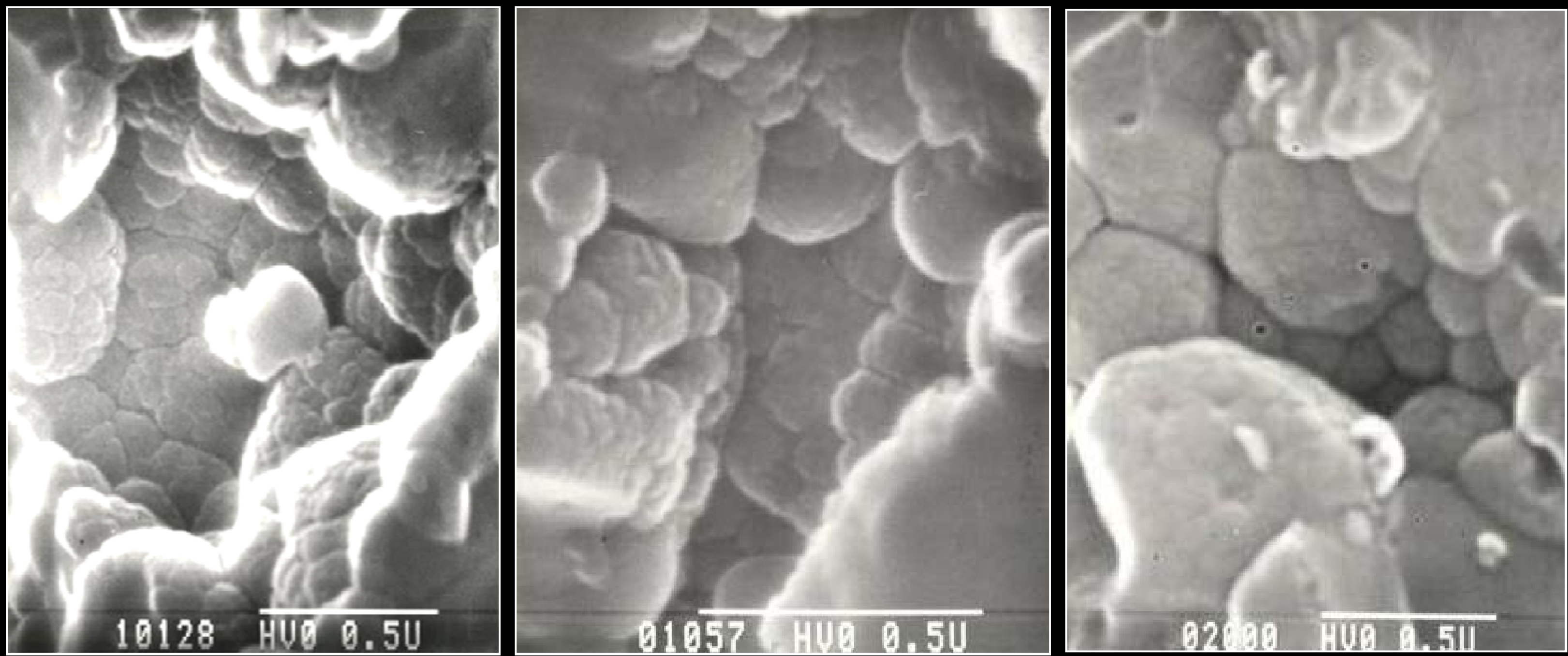

# Coulomb explosion (Fleisher, Price, Walker, 1965)

Commission européenne

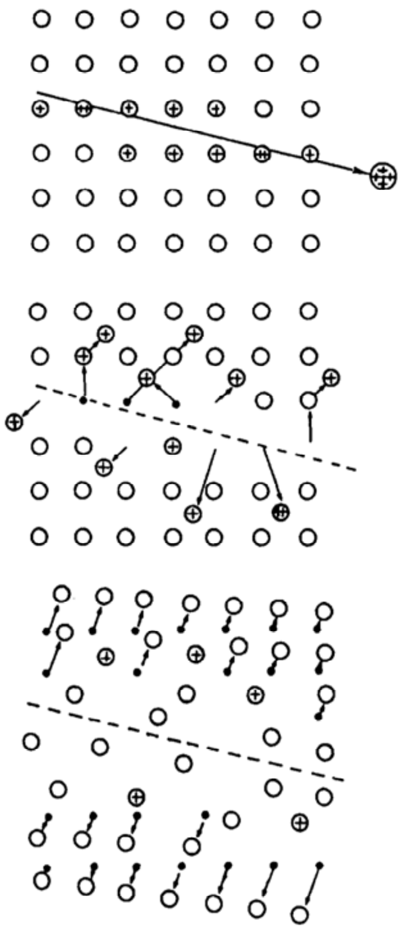

Ionization

Electrostatic displacement

Relaxation and elastic strain

Depends strongly on the primary ionization, on the lattice binding forces.

But also...
on the electron mobility
→ Insulators most sensitive

# SEM of a 200 GWd / $t_U$ fuel sample

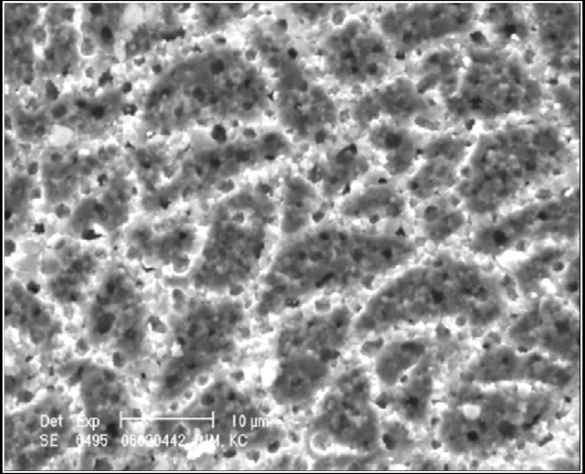


Memory effect after HBS formation

**5000 dpa**

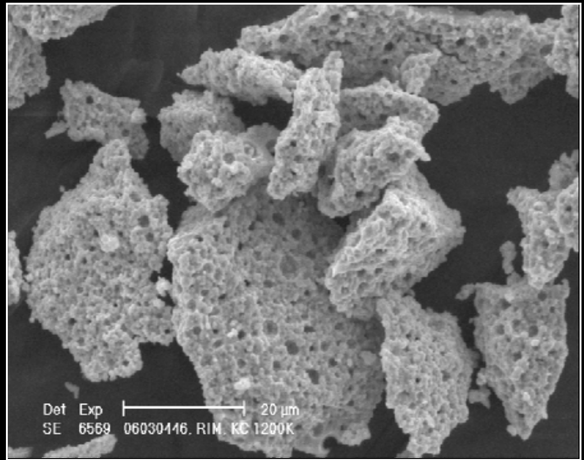


Break of the structure during annealing (1200 K)

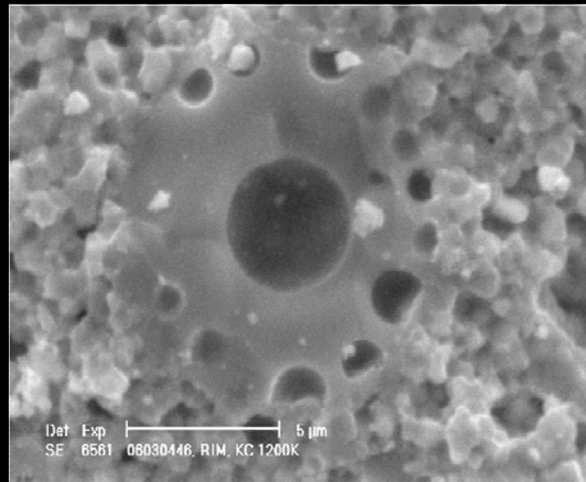


Formation of „ultimate“ pores at very high burnup

**Fission product release and microstructure changes during laboratory annealing of a very high burn-up fuel specimen,**
**J.-P. Hiernaut *, T. Wiss, J.-Y. Colle, H. Thiele, C.T. Walker, W. Goll, R.J.M. Konings, J.Nucl. Mater., 2008, Journal of Nuclear Materials 377 (2), pp. 313-**

# Release of volatile FPs vs BU

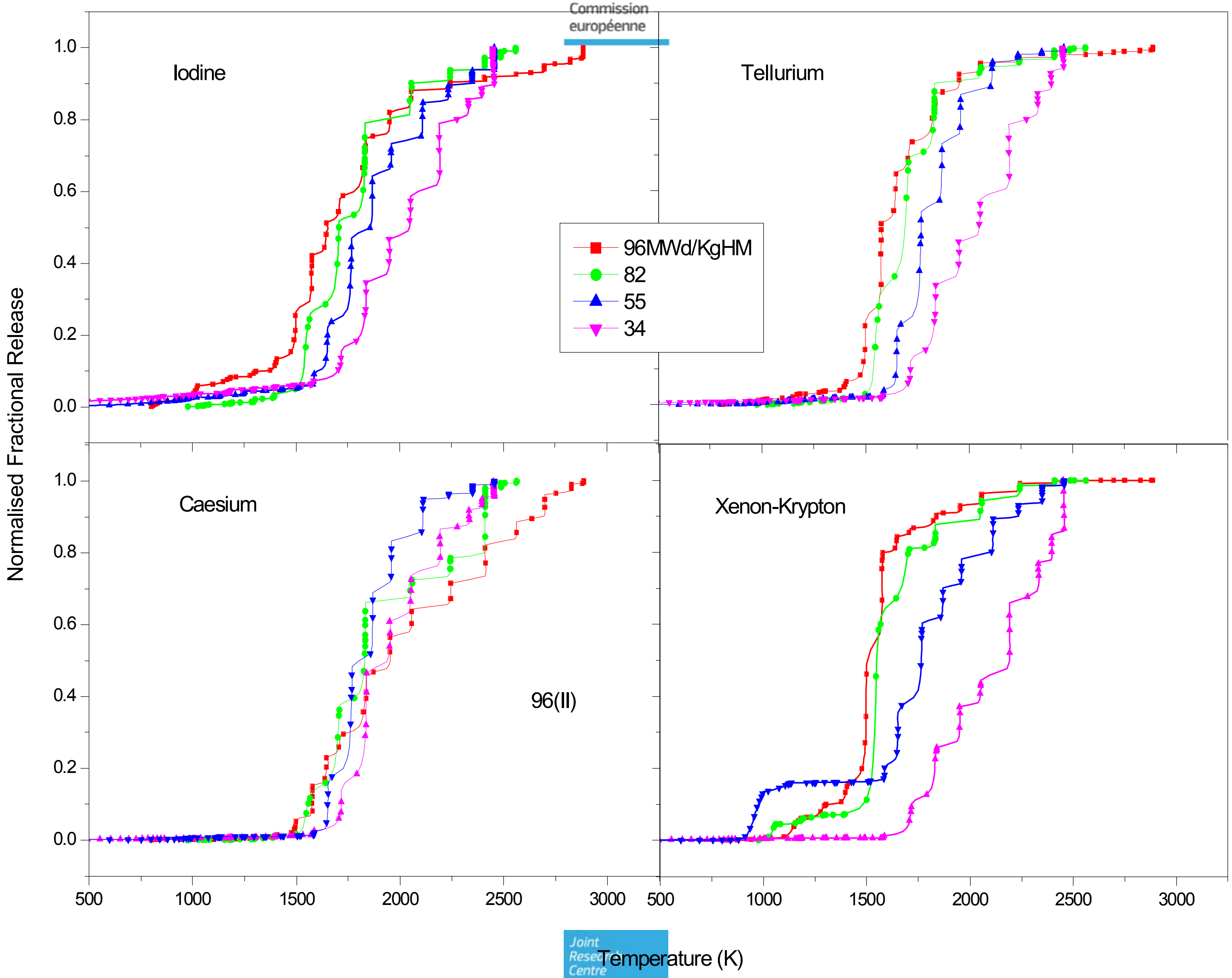


Commission européenne
Joint Research Centre

# Fission gas Release in irr. $UO_2$

Commission européenne

A burnup and temperature matrix has been used to determine the threshold for fission gas release

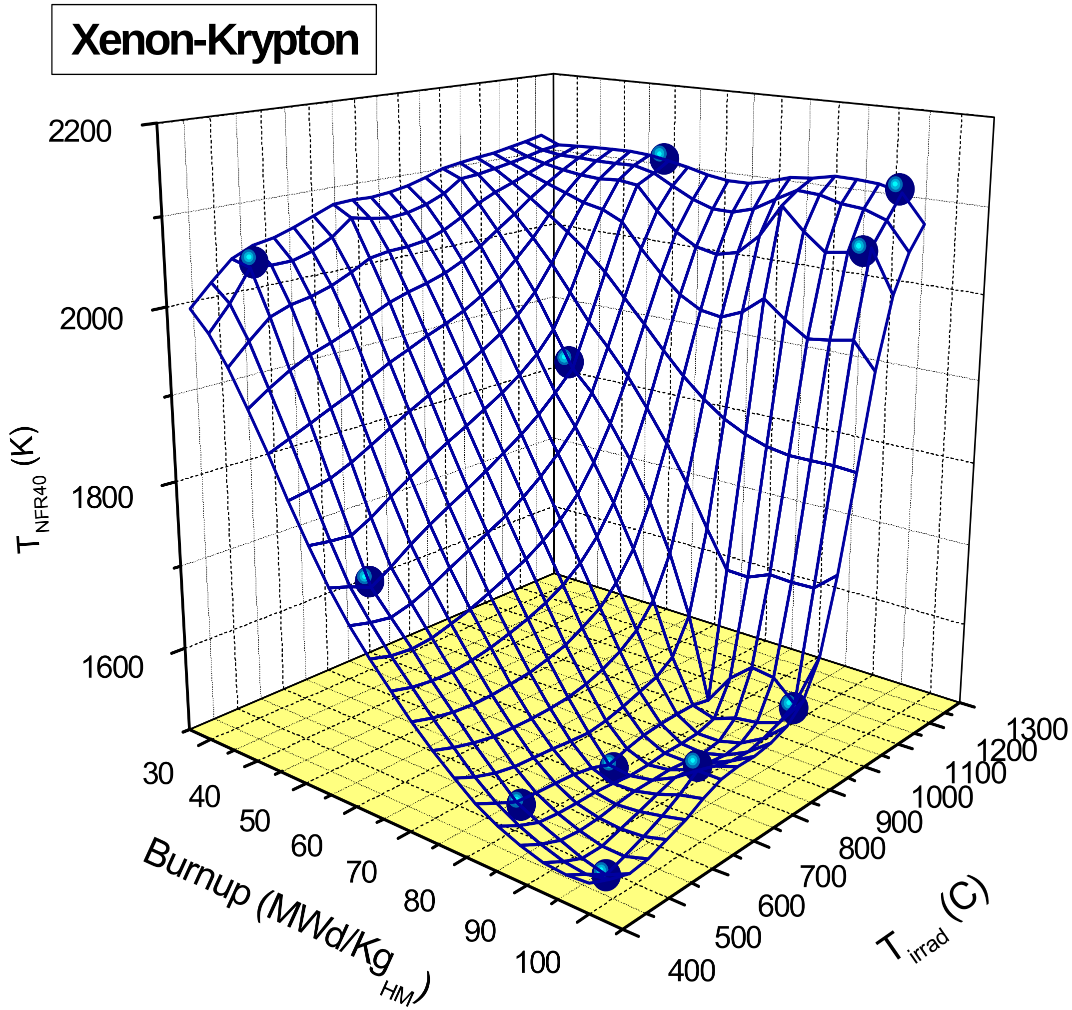


To be submitted to JNM in, "Release of volatile fission products during thermal annealing of LWR UO2 fuel irradiated of different burnup and temperature"

By J.-P. Hiernaut, T. Wiss, J. Spino, V.V. Rondinella, R.M.J. Konings, T Sonoda, M. Kinoshita

Joint Research Centre

# TEM analysis of $(U_x, Th_y, Pu_z)O_2$

$(U_{0.9}, {}^{238}Pu_{0.1})O_2$

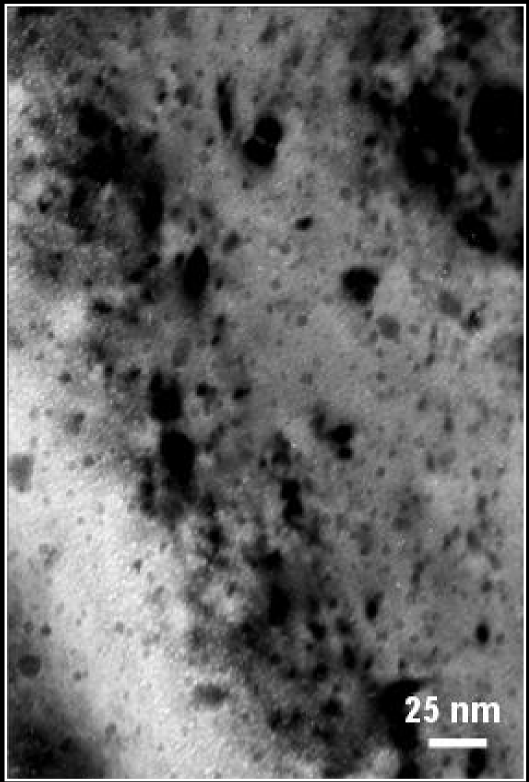


1.7·10[18] He.g[-1]

0.7 dpa

T = 2 y

$({}^{238}Pu_{0.9}, Pu_{0.1})O_2$


$3.6\cdot10^{20}$ He.g$^{-1}$

100 dpa

T = 30 y

$(U_{0.33},Th_{0.67})O_{2+y}$


$7.2\cdot10^{20}$ He.g$^{-1}$

170 dpa

T = $550\cdot10^{6}$ y

NF PRO

# PIE of fuel

Large damage ingrowth

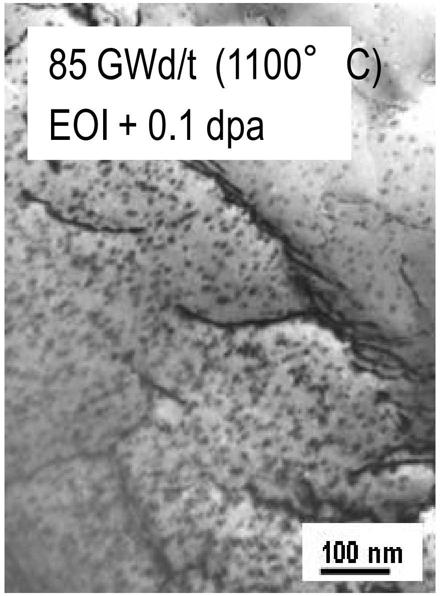


Irradiated fuel

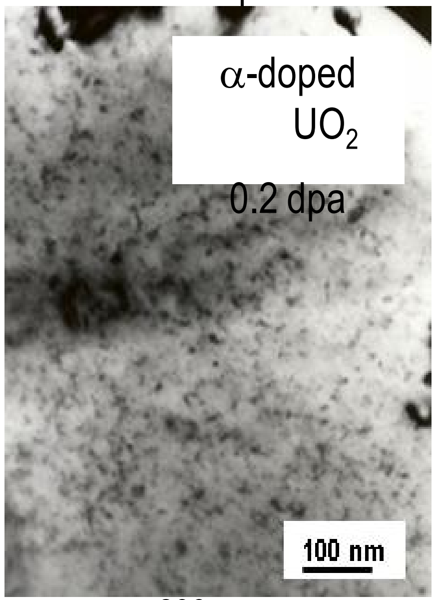


$(U_{0.9}, {}^{238}Pu_{0.1})O_2$

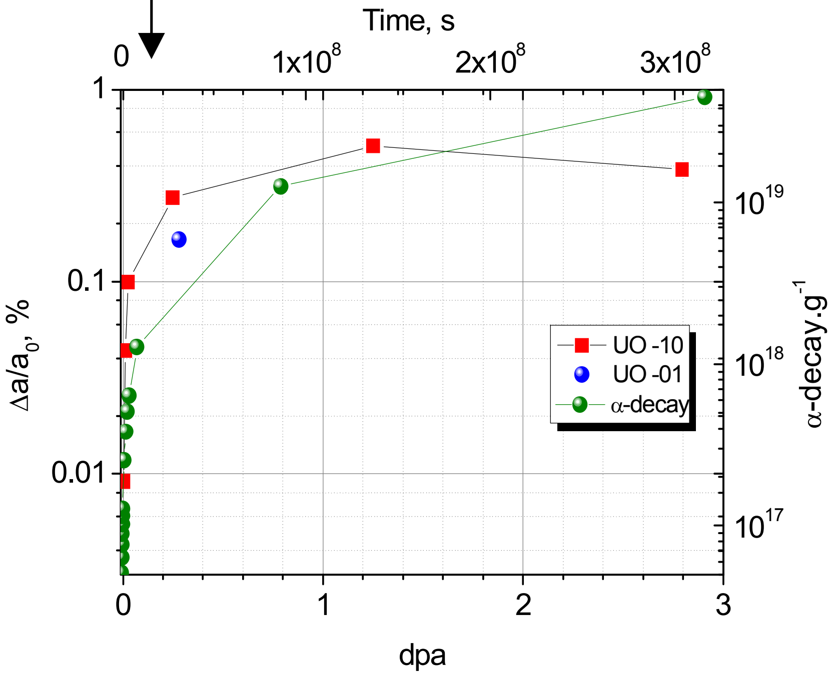


Can HBS be explained by these observations ?

# Swelling of $MgAl_2O_4$ IMF

Commission européenne

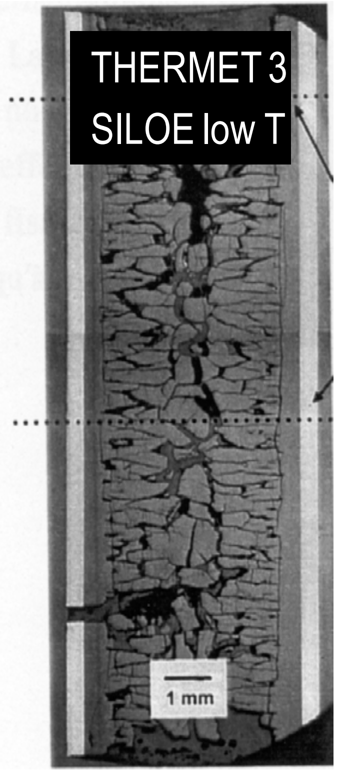


Microdispersed

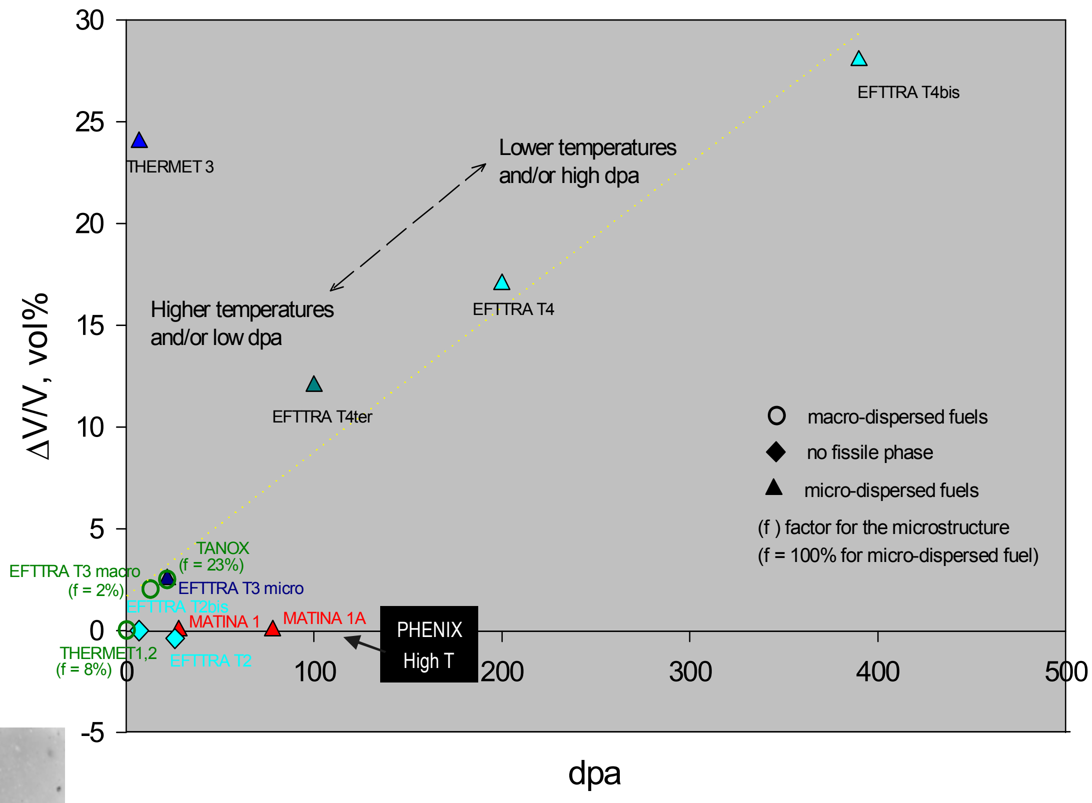


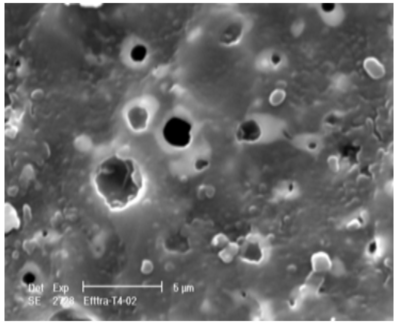

EFTTRA-T4

HFR

EFTTRA-T3 macro


Macrodispersed

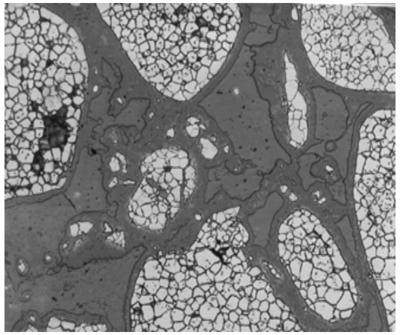

Joint Research Centre

# Fission induced gas release

Commission européenne

**Implantation of $^{85}Kr$**

**Subsequent irradiation with 72 MeV iodine-ions**

The radiation-enhanced diffusion coefficient, D*, varied linearly with the fission rate, F, according to the relation

D*=AF with A=1.2x10$^{-29}$ cm$^5$ and F in fissions/sec ·cm³.

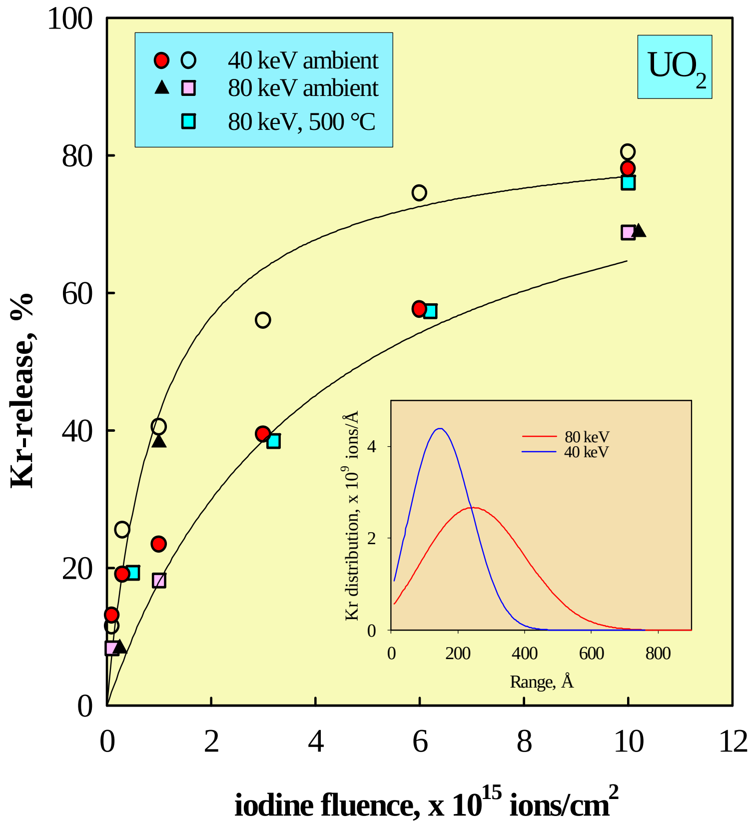


Joint Research Centre

# Behaviour of gas in solids



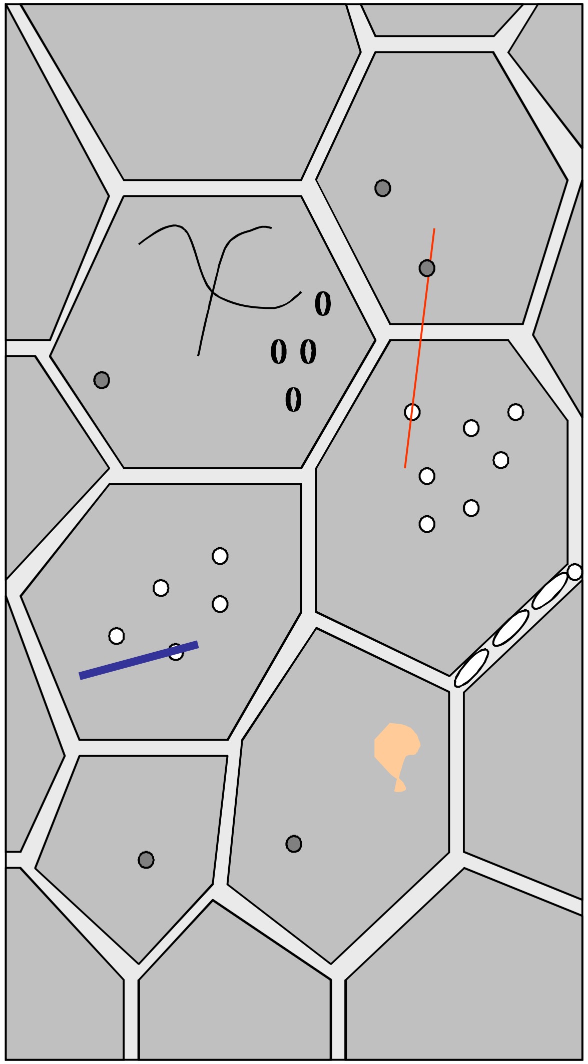

Fundamental data
thermodynamic solubility, diffusion coefficients

Influence of: grain boudaries, bubble formation, radioactive decay, fission, temperature, gas re-solution, impurities, microstructure,..

On: gas mobility, release, material property changes (mechanical, integrity, thermo-physical)

Concerns: Spent fuel, operating fuels, waste conditioning matrices, IM.

# Criteria for stability

Commission européenne

The ionicity criterion
Cubic structure are underlined

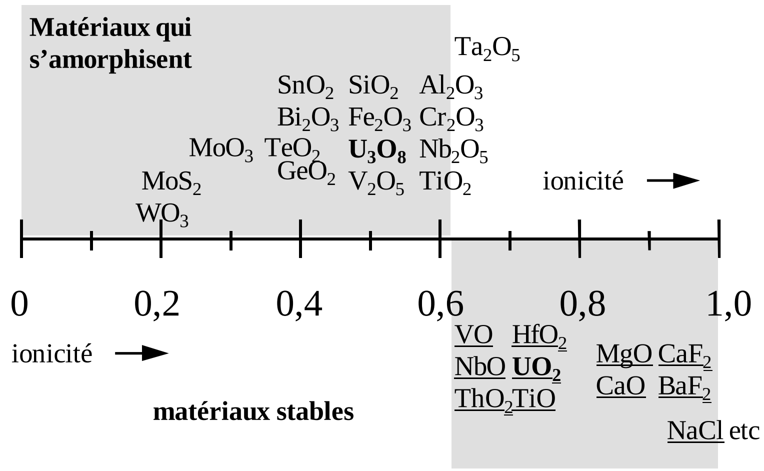


Crystallization temperature criterion

H.M. Naguib and R. Kelly

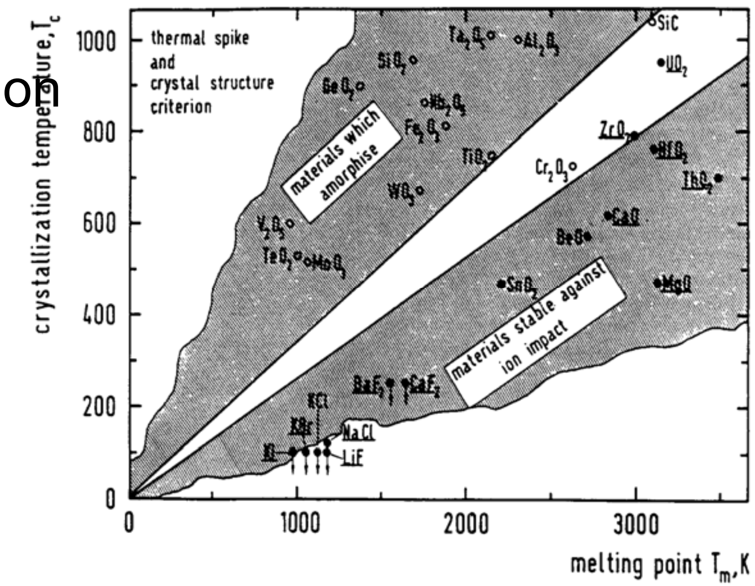

# Lattice defects from radiation damage

defect clusters in ion-irradiated $UO_2$

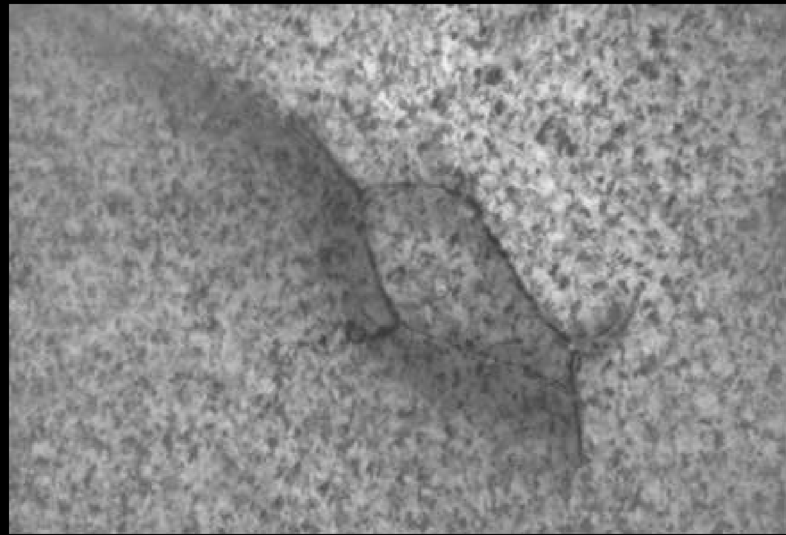

Dislocation loops in $UO_2$ irradiated at 800 K

100 nm ⟷

Dislocations in $UO_2$ irradiated at 1300 K

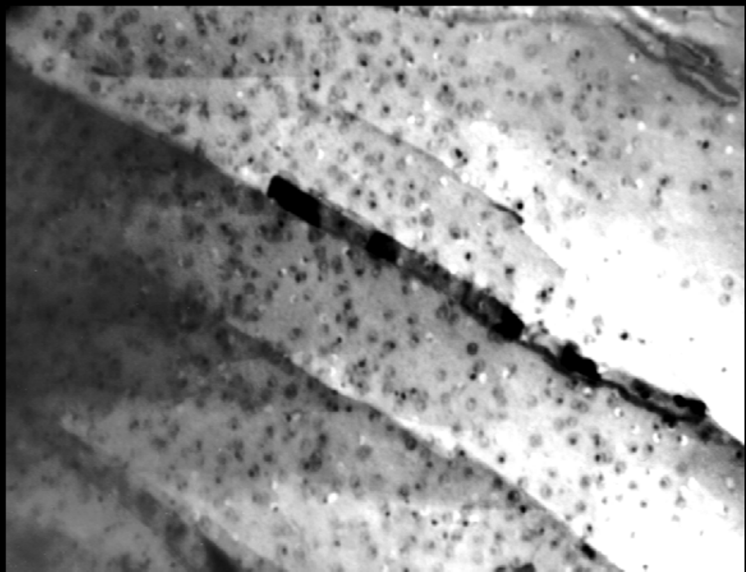

# Thermal spike model of *Toulemonde*

Commission européenne

$$Ce\frac{\partial Te}{\partial t} = \nabla(Ke\nabla Te) - g(Te - T) + \frac{B(r,t)}{Ce}$$

$$\rho C(T)\frac{\partial T}{\partial t} = \nabla(K(T)\nabla T) + g(Te - T)$$

g : electron-phonons coupling constant ($W.cm^{-3}.K^{-1}$)
$C_e$ : electron specific heat (J.cm-3.K-1).
C : material specific heat (J.g-1.K-1).
T : lattice temperature (K).
$T_e$ : electronic temperature (K).

The equations describe the heating and cooling of the electronic system and the atomic system respectively.

The term $B(r,t)/C_e$ is the energy deposited to the material ($UO_2$) by one ion from the ion-beam.

The equation system is not solved analytically but a numerical solution can be calculated with only one free parameter, i.e. the mean diffusion length of the energy on the electrons. For the case of $UO_2$ based on the TEM observations of tracks a value of 6 nm is found.
Tracks of 3 nm diameter could be expected for a heavy fission fragment (full energy).

**No direct observation of tracks in fuel but athermal diffusion and creep and gas bubble re-solution.**

Joint Research Centre

# Apparent Specific Heat during annealing

Commission européenne

## Analysis of the heat effects

The reaction-rate formalism can be used to calculate the **i**nterstitial and **v**acancy concentrations :

$$K - D_i c_i k_i^2 - \alpha c_i c_v = \frac{dc_i}{dt}$$

$$K' - D_v c_v k_v^2 - \alpha c_i c_v = \frac{dc_v}{dt}$$

Simple model for defect annealing : each kind of defects is a single-energy activated process and the reaction (recombination or precipitation) is supposed to obey a reaction-rate equation of type:

$$\frac{dc}{dt} = -kc^2$$

*c* is the spatial concentration of the involved defects or defect/antidefect pairs, and *k* is a characteristic time related to the mobility of the faster defect, and expressed as:

$$k = KD_0 e^{-\frac{H}{RT}}$$

4 parameters for each process:

$C_0$ (initial concentration): deduced from the previous experiments
H (diffusion enthalpy)
K $D_0$ (reaction constant)
E (recovered energy during annealing): deduced from the observed heat effect & literature

# Sample description – Main results

| sample | Original composition | Age, y | Damage, dpa | He, at.g$^{-1}$ | Bubbles | | Bubble pressure, MPa | Swelling, % | |
|---|---|---|---|---|---|---|---|---|---|
| | | | | | Average radius, nm | Conc., m$^{-3}$ | | lattice | From bubbles |
| UO233 | $(U_{0.9}{}^{233}{}_{U0.1})O_2$ | 5 | 0.00001 | $3.8x10^{14}$ | | | | **0.09** | |
| UO01 | $(U_{0.999}{}^{238}Pu_{0.001})O_2$ | 9 | 0.028 | $7.6x10^{16}$ | | | | **0.5** | |
| MOX40 | $(U_{0.6}{}^{239}Pu_{0.4})O_2$ | 12 | 0.12 | $4.7x10^{17}$ | | | | **0.7** | |
| UO10 | $(U_{0.9}{}^{238}Pu_{0.1})O_2$ | 9 | 2.8 | $7.6x10^{18}$ | **1.2** | **$1.5x10^{22}$** | | **1.3** | **0.01** |
| $P^3B$ | $({}^{238}Pu_{0.9}, Pu_{0.1})O_2$ | 30 | 100 | $3.6x10^{20}$ | **2.5** | **$5x10^{23}$** | 180 | **2.2** | **3** |
| RTG | ${}^{238}PuO_2$ | 36 | 110 | $5.5x10^{20}$ | | | | | |
| T4 | $(U_{0.33},Th_{0.67})O_{2+y}$ | $550x10^6$ | 170 | $7.2x10^{20}$ | **3** | **$8x10^{23}$** | 320 | 1.5 | **9** |
| U2 | $(U_{0.92},Th_{0.08})O_{2+y}$ | $220 x10^6$ | 130 | $5.8x10^{20}$ | | | | 1.5 | |

Nb: the van der Waals equation of state has not been used to calculate $P_{bubble}$